B. Castellano López and M. Nieto-Sampedro (Eds.)
Progress in Brain Research, Vol. 132

CHAPTER 28

Glial diffusion barriers during aging and pathological states

Eva Syková *

Department of Neuroscience, 2nd Medical Faculty, Charles University and Institute of Experimental Medicine, Academy of Sciences of the Czech Republic, Vídeňská 1083, 14220 Prague 4, Czech Republic

Introduction

Glial cells do not communicate by synaptic transmission, do not form synapses and interact with neurons by diffusion of ions, transmitters and other neuroactive substances through the extracellular space (ECS). The ECS of the central nervous system (CNS) is the microenvironment of the neurons and glia, and an important communication channel (Syková, 1983, 1992, 1997; Nicholson and Syková, 1998). It includes ions, transmitters, metabolites, peptides, neurohormones and molecules of the extracellular matrix, which directly or indirectly affects neuronal and glial cell functions. Neurons and glia release a number of neuroactive substances, which diffuse via the ECS to their targets located on nerve and glial cells, frequently distant from the release sites.

Glial cells communicate by extrasynaptic (volume) transmission

Transmitters which are released non-synaptically diffuse through the ECS and bind to extrasynaptic, usually high-affinity, binding sites located on neurons, axons and glial cells. This type of extrasynaptic transmission is also called 'diffusion transmission' (neuroactive substances diffuse through the ECS) or 'volume transmission' (neuroactive substances move through the volume of the ECS) (Fuxe and Agnati, 1991; Agnati et al., 1995; Syková, 1997; Nicholson and Syková, 1998; Zoli et al., 1999). This mode of communication without synapses provides a mechanism for long-range information processing in functions such as vigilance, sleep, chronic pain, hunger, depression, LTP, LTD, memory formation and other plastic changes in the CNS (Syková, 1997). Populations of neurons can interact both synaptically and by the diffusion of ions and neurotransmitters through the ECS, while glial cell signaling is always extrasynaptic.

Extrasynaptic transmission is critically dependent on the structure and physicochemical properties of the microenvironment–ECS. These properties vary, around each cell and in different regions of the brain. Certain synapses ('private synapses') or even whole neurons are tightly ensheathed by glial processes and by the extracellular matrix forming so-called 'perineuronal nets' (Celio et al., 1998), others are left 'naked'. Molecules from the ECS can access these 'open' synapses more readily (Fig. 1). On the other hand, transmitters, e.g. glutamate or GABA, can escape from the synaptic cleft (especially during repetitive stimulation or massive release of a transmitter) and affect the extrasynaptic receptors on glia or neurons or reach another synapse. These phenomena have been termed 'transmitter spillover' and 'cross-talk' between synapses (Kullmann et al., 1996; Asztely et al., 1997). The size and irregular geometry of diffusion channels in the ECS (tissue tortuosity and anisotropy) substantially differ in various CNS regions and thus affect and/or direct the

* Corresponding author: E. Syková, Department of Neuroscience, Institute of Experimental Medicine ASCR, Vídeňská 1083, 142 20 Prague 4, Czech Republic. Tel.: +420-2-475-2204; Fax: +420-2-475-2783;
E-mail: sykova@biomed.cas.cz

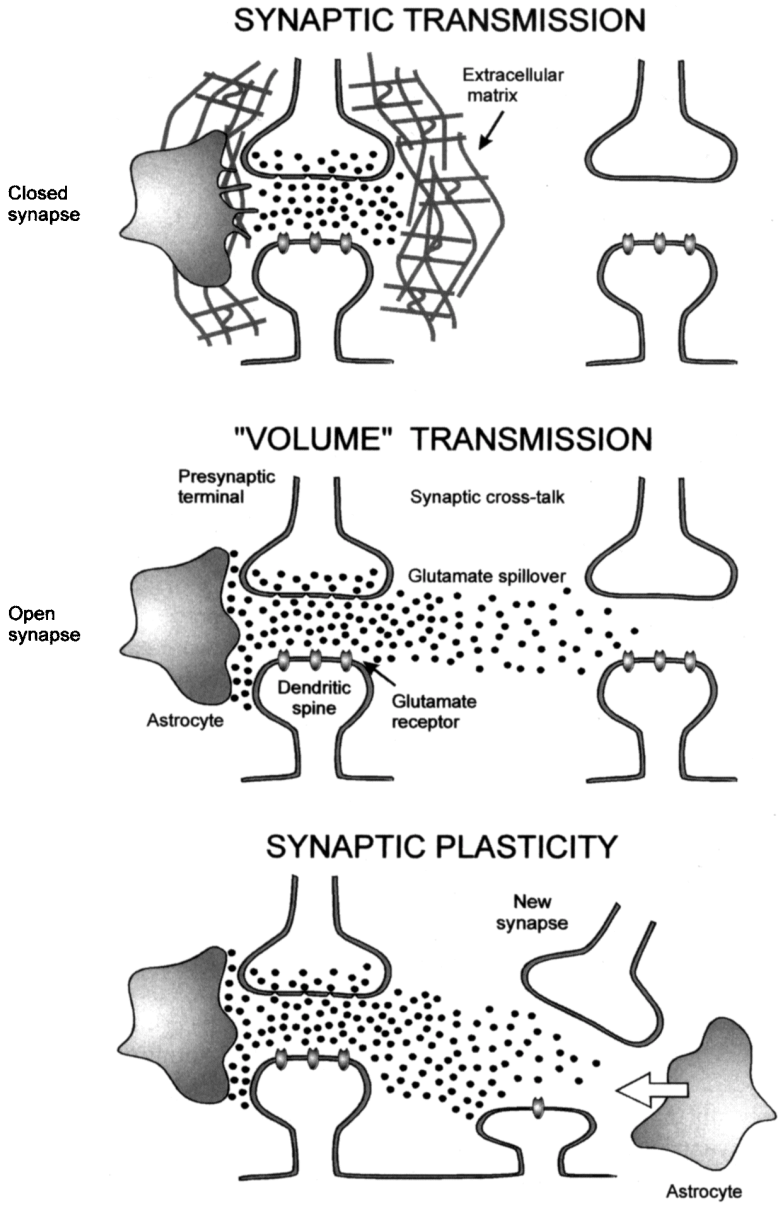

Fig. 1. Concept of synaptic transmission and extrasynaptic volume transmission. Closed synapses are typical of synaptic transmission. This synapse is tightly ensheathed by glial processes and extracellular matrix forming perineuronal or perisynaptic nets. Open synapse is typical of volume transmission. It allows the escape of transmitter (e.g. glutamate, GABA) from the synaptic cleft (spillover), diffusion in ECS and binding to receptors on nearby synapse. This phenomenon is known as 'cross-talk' between synapses. The spillover may also lead to plastic changes, inducing formation of new synapses, or eliciting the rearrangement of astrocytic processes around the synapse.

movement of various neuroactive substance. Diffusion parameters thereby modulate neuronal signaling, neuron–glia communication and extrasynaptic 'volume' transmission. During glial cell maturation, proliferation, hypertrophy and swelling, changes occur in ECS ionic composition, extracellular matrix, ECS volume, ECS geometry and neuronal loss. Diffusion parameters are also altered during develop-

ment, aging, CNS injury, anoxia/ischemia, spreading depression, inflammation, demyelination, in tumors and many other brain pathological states.

Role of glia in ECS ionic and volume homeostasis

Cellular elements and blood vessels fill about 80% of the total CNS tissue volume and the remaining portion (about 20%) is the ECS. ECS ionic changes resulting from transmembrane ionic shifts during neuronal activity depolarize neighboring neurons and glial cells, enhance or depress their excitability, and affect ion channel permeability (Syková, 1983; Walz, 1989; Chesler, 1990; Syková, 1992; Deitmer and Rose, 1996; Syková, 1997; Ransom, 2000). These ionic changes may also lead to the synchronization of neuronal activity and stimulate glial cell function.

The ionic composition of the ECS in the brain closely matches the composition of the cerebrospinal fluid. The introduction of ion-sensitive microelectrodes (ISM) with a liquid ion-exchanger for K^+, and later for other ions (e.g. Cl^-, H^+, Ca^{2+}), made it possible to follow the dynamic extracellular and intracellular ionic changes during neuronal activity in the normally functioning CNS as well as during pathological states (for reviews see Syková, 1983, 1992, 1997). Ionic and volume homeostasis in the CNS is maintained by a variety of mechanisms present in neurons as well as in glial cells. It was shown in a number of studies in vivo as well as in vitro that changes in extracellular K^+ concentration ($[K^+]_e$), alkaline and acid shifts in pH_e and decreases in extracellular Ca^{2+} concentration ($[Ca^{2+}]_e$) accompany neuronal activity in different brain regions (for review see Syková, 1983, 1992; Chesler, 1990).

The redistribution of activity-related ionic changes is mediated, at least partially, by the Na^+, K^+-ATPase transport mechanism, which is located in neurons as well as in glial cells. Besides the Na^+/K^+ pump activity, K^+ homeostasis in the ECS is also maintained by three other mechanisms located in glial cells: (1) K^+ spatial buffering; (2) KCl uptake; and (3) Ca^{2+}-activated K^+ channels.

pH changes in the ECS result from both neuronal and glial cell activity. There is now convincing evidence for the neuronal origin of extracellular alkaline shifts and the glial origin of activity-related acid shifts (for review see Syková, 1997). Glial cells play an important role in buffering activity-related alkaline changes in extracellular pH. Some membrane transport processes regulating intra- and extracellular pH, such as Na^+/H^+ exchange and $Na^+/H^+/Cl^-/HCO_3^-$ cotransport, are present in both neurons and glia, while others are specific either for neurons (e.g., H^+ channels, H^+ or HCO_3^- permeability of the ionic channels opened by GABA or glutamate) or for glia (e.g., the voltage-dependent Na^+-HCO_3^- cotransport and lactate extrusion). The glial cell membrane is also readily permeable to CO_2, which reacts with H_2O to form carbonic acid, which in turn quickly dissociates into water and protons. This reaction is enhanced by the catalytic action of the enzyme carbonic anhydrase, which is almost exclusively present in glial cells. Some of the membrane transport mechanisms result in alkaline shifts in pH_e (acid loaders), while others result in acid shifts in pH_e (acid extruders), but it is evident that acid loaders are dominant in neurons, while acid extruders are dominant in glia (Syková, 1992; Chesler, 1990; Deitmer and Rose, 1996). Extracellular acid shifts are, therefore, a consequence of activity-related $[K^+]_e$ increase. K^+-induced glial depolarization results in an alkaline shift in glial pH_i, which leads to the stimulation of classical acid extrusion systems in glial cells. Membrane mechanisms responsible for the transport of ions across the cell membrane are always accompanied by the movement of water, thus affecting the cell volume and thus the size and tortuosity of the ECS (Fig. 2). However, in immature animals such as 3–5-day-old rats the ECS is much larger than in adults (Lehmenkühler et al., 1993; Prokopová et al., 1997) and this may be one of the reasons why the decrease in pH_e (acid shift) is smaller and delayed and neuronal activity is not suppressed (Fig. 2).

During early postnatal development, when glial cell function is incomplete, activity-related pH_e and $[K^+]_e$ changes are substantially different from those observed in adult animals with completed gliogenesis and glial cell function. In the neonatal rat spinal cord, stimulation-evoked changes in $[K^+]_e$ are much larger than in the adult animal (Fig. 3) (Jendelová and Syková, 1991). In newborn rats, alkaline shifts dominate in the ECS, as the acid shifts generated by glia are small. At postnatal day 10, when gliogenesis in rat spinal cord gray matter peaks, the K^+ ceiling

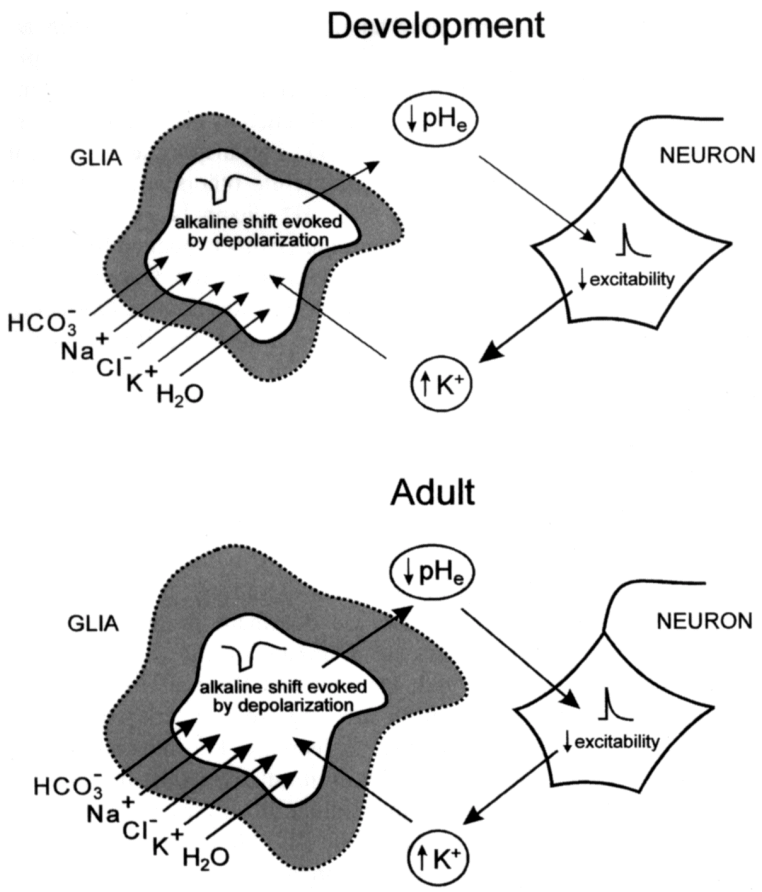

Fig. 2. Schematic of the mechanism of non-specific feedback suppressing neuronal excitability in developing and adult brains. Active neurons release K^+, which accumulates in the ECS, depolarizes glial cells and is taken up by glia. In depolarized glial cells, an alkaline shift is evoked by activation of Na^+/HCO_3^- cotransport. This alkaline shift in glial pH_i causes an acid shift in pH_e. Extracellular acidosis further suppresses neuronal activity. Transmembrane ionic movements are accompanied by water and will therefore result in glial swelling (greater and faster in adult brain). ECS volume decreases lead to a greater accumulation of ions and neuroactive substances and to a 'crowding' of molecules in the extracellular matrix of the ECS.

level decreases and stimulation evokes acid shifts in the range of 0.1–0.2 pH unit (Fig. 3A,B), which are preceded by scarcely discernible alkaline shifts, also observed in adult rats. Stimulation-evoked alkaline shifts are, in addition, abolished by the blockage of synaptic transmission by Mn^{2+} or Mg^{2+}, while acid shifts are unaffected (Syková et al., 1992). Similar results were observed in chicks, in which light stimulation or the application of the bitter tasting substance methylantranilate (MeA) resulted in alkaline shifts in pH_e in hyperstriatum ventrale of the brain in 3-day-old chicks. It was not until 10 days after hatching that an acid shift replaced the alkaline (Fig. 3C), suggesting that glial cells are functionally mature at this stage (Ng et al., 1991). Alkaline shifts resulting from neuronal activity are depressed by the application of the GABA antagonist picrotoxin and by glutamate receptor antagonists and channel blockers such as MK801 (non-competitive NMDA receptor antagonist and channel blocker) and CNQX (competitive AMPA/kainate receptor antagonist) (Syková et al., 1992; Jendelová et al., 1994). Glial cells in adult brains play an important role in buffering activity-related alkaline changes in extracellular pH. This so-called mechanism of negative feedback control suppresses neuronal excitability (Fig. 2).

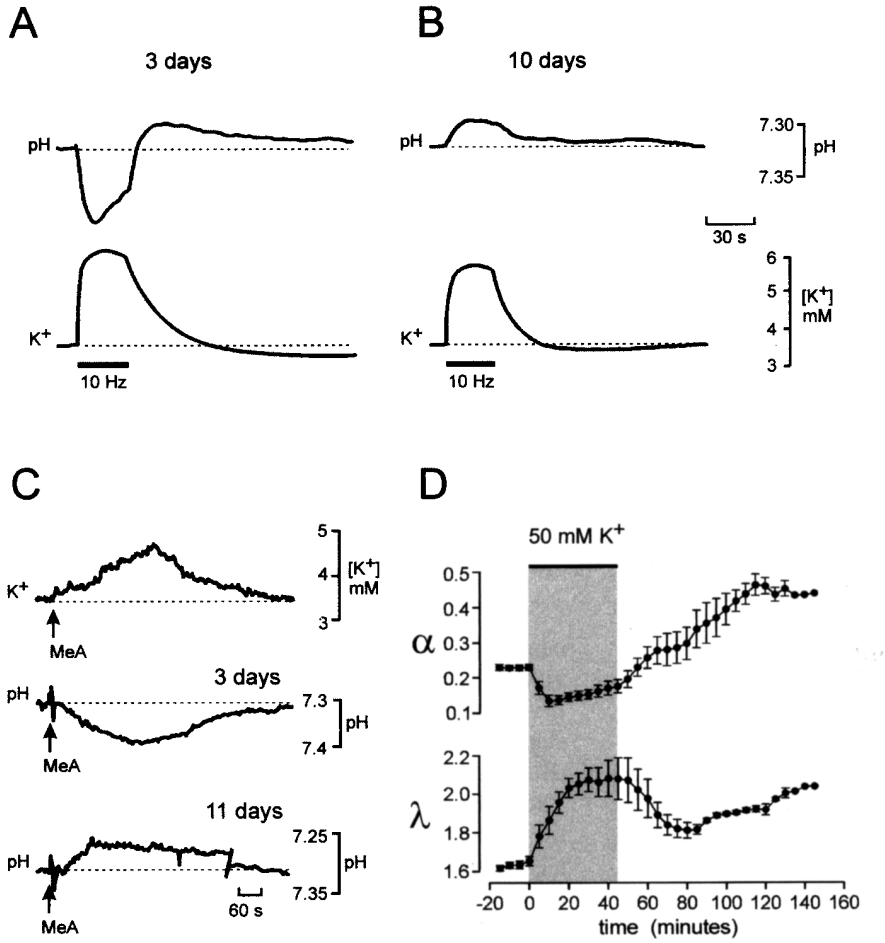

Fig. 3. Stimulation-evoked $[K^+]_e$ and pH_e changes during early postnatal development. (A) Repetitive electrical stimulation of the dorsal root in 3-day-old rats was accompanied by an alkaline shift and by an increase in $[K^+]_e$. When stimulation was discontinued, a poststimulation acid shift of smaller amplitude appeared, which was accompanied by a K^+-undershoot. (B) In the 10-day-old rat the $[K^+]_e$ increase was smaller and was accompanied by an extracellular acid shift. (C) The effect of taste aversant methylantranilate (MeA) placed on the tongue of anesthetized chicks on $[K^+]_e$ and pH_e recorded in the hyperstriatum ventrale at postnatal days 3 and 11. In 3-day-old chicks MeA evoked an alkaline shift, while in 11-day-old chicks, only an acid shift was detected. (D) The effect of 50 mM K^+ on extracellular space diffusion parameters in spinal cord gray matter as measured in 10–13-day-old rats. Each data point represents mean ± S.E.M., calculated from α and λ values recorded at 5-min intervals ($n = 7$). Note that initially the α decreased and λ increased; however, during application, α returned towards control values, possibly due to regulatory volume decrease (RVD), while λ remained either unchanged or increased further. During washout of 50 mM K^+ α overshot control values and λ showed a second increase, associated with astrogliosis (not shown).

Diffusion of substances in the ECS, ECS volume and tortuosity

The diffusion of substances in a free medium, such as water or diluted agar, is described by Fick's laws. In contrast to a free medium, diffusion in the ECS of nervous tissue is hindered by the size of extracellular clefts, the presence of membranes, fine neuronal and glial processes, macromolecules of the extracellular matrix, charged molecules, and by cellular uptake (Fig. 4). To allow for these factors, it was necessary to introduce three ECS diffusion parameters and modify Fick's original diffusion equations (Nicholson and Phillips, 1981; Nicholson

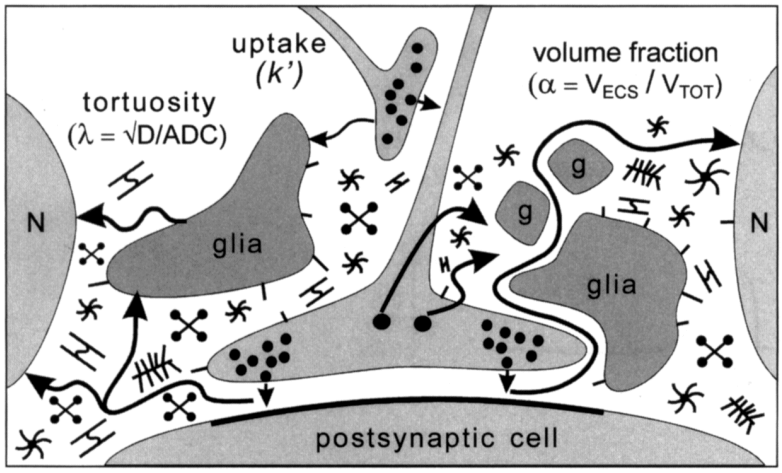

Fig. 4. Schematic of CNS architecture. The CNS architecture is composed of neurons (N), axons, glial cells (glia), cellular processes (G), molecules of the extracellular matrix and intercellular channels between cells. This architecture slows the movement (diffusion) of substances in the brain, which is critically dependent on the ECS diffusion parameters volume fraction (α), tortuosity (λ) and non-specific uptake (k').

and Syková, 1998). First, diffusion in the CNS is constrained by the restricted volume of the tissue available for the diffusing particles, i.e. by the extracellular space volume fraction (α), which is a dimensionless quantity and is defined as the ratio between the volume of the ECS and the total volume of the tissue ($\alpha = V_{ECS}/V_{TOT}$). It is now evident that the ECS in the adult brain amounts to about 20% of the total brain volume, i.e. $\alpha = 0.2$. Second, the free diffusion coefficient (D) in the brain is reduced by the tortuosity factor (λ). ECS tortuosity is defined as $\lambda = (D/ADC)^{0.5}$, where D is a free diffusion coefficient and ADC is the apparent diffusion coefficient in the brain. As a result of tortuosity (in adult brain λ amounts to 1.55–1.65), D is reduced to an apparent diffusion coefficient $ADC = D/\lambda^2$. Thus, any substance diffusing in the ECS is hindered by many obstructions. Third, substances released into the ECS are transported across membranes by non-specific concentration-dependent uptake (k'). In many cases, however, these substances are transported by energy-dependent uptake systems that obey non-linear kinetics (Nicholson, 1995). When these three factors (α, λ and k') are incorporated into Fick's law, diffusion in the CNS is described satisfactorily (Nicholson and Phillips, 1981).

The real-time iontophoretic method is used to determine ECS diffusion parameters and their dynamic changes in nervous tissue in vitro as well as in vivo (Syková, 1997; Nicholson and Syková, 1998). In principle, ISM are used to measure the diffusion of ions to which the cell membranes are relatively impermeable, e.g. TEA^+, TMA^+ or choline. These substances are injected into the nervous tissue by pressure or by iontophoresis from an electrode aligned parallel to a double-barreled ISM at a fixed distance (Fig. 5). Such an electrode array is made by gluing together a pressure or iontophoretic pipette and a TMA^+-sensitive ISM with a tip separation of 60–200 μm. In the case of iontophoretic application, TMA^+ is released into the ECS by applying a current step of +80–100 nA with a duration of 40–80 s. The released TMA^+ is recorded with the TMA^+-ISM as a diffusion curve (Figs. 5 and 6), which is then transferred to a computer. Values of the ECS volume, ADCs, tortuosity and non-specific cellular uptake are extracted by a non-linear curve-fitting simplex algorithm applied to the diffusion curves.

Other methods used to study ECS volume and geometry, including tissue resistance, integrative optical imaging (IOI), nuclear magnetic resonance (NMR) and intrinsic optical signals (IOS) are less comprehensive because they measure only relative changes in the ECS diffusion parameters or only some of the three diffusion parameters (Van Harreveld et al., 1971; Matsuoka and Hossmann, 1982;

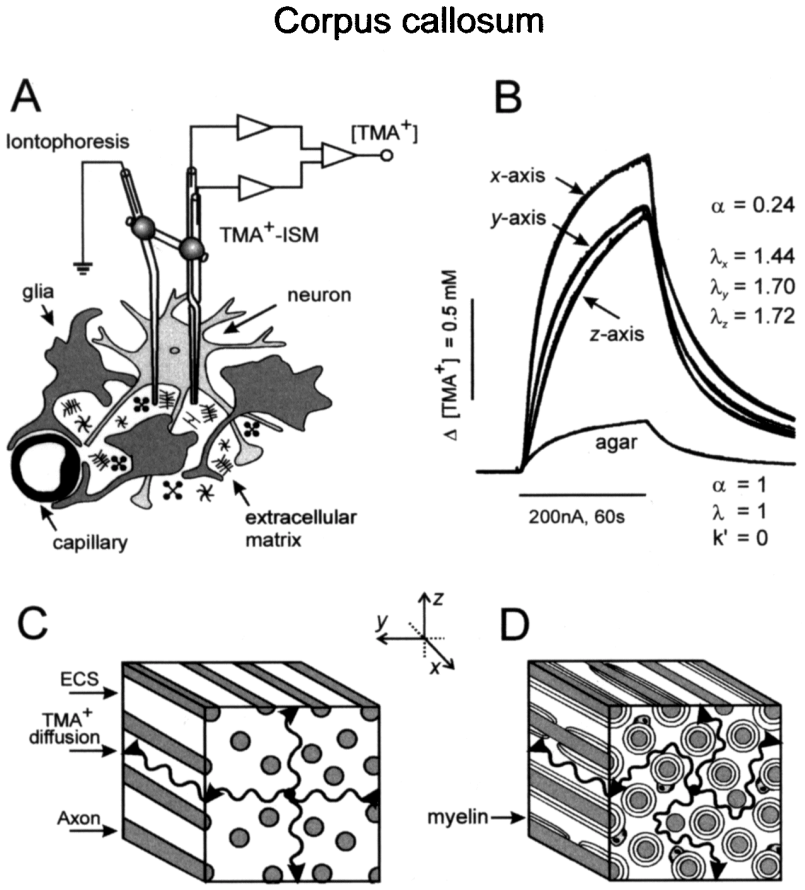

Fig. 5. Experimental set-up, TMA^+ diffusion curves and typical ECS diffusion parameters α (volume fraction) and λ (tortuosity) obtained in the white matter of the CNS (corpus callosum, CC). (A) Schematic of the experimental arrangement. A TMA^+-selective double-barreled ion-selective microelectrode (ISM) was glued to a bent iontophoresis microelectrode. The separation between electrode tips was 130–200 μm. (B) Typical TMA^+ diffusion curves obtained in agar and in CC made in three orthogonal axes (x, y and z) showing anisotropic diffusion. The x-axis lies along the axons while the y- and z-axes lie across the fibers. All recordings are from the same animal at P21. The slower rise in the z than in the y direction and in the y than in the x direction indicates a higher tortuosity and more restricted diffusion. Actual ECS volume fraction α is about 0.2 and can be calculated only when measurements are done along the x-, y- and z-axes. Recordings were first made in agar, where by definition $\alpha = 1 = \lambda$ and $k' = 0$, and the electrode transport number (n) and diffusion coefficient of the TMA^+ (D) are extracted by curve fitting. Knowing n and D, the parameters α, λ, and k' were obtained in all three axes in CC. The shape and amplitude of the diffusion curves reflect the different apparent diffusion coefficients (*ADC*s), i.e. λ values, associated with each axis. (C,D) Schematic representation of substance diffusion in the ECS of unmyelinated white matter (isotropic diffusion) and myelinated white matter (anisotropic diffusion). (D) Movement of substances is faster along the myelinated axons than in the direction perpendicular to them.

Korf et al., 1988; Nicholson and Tao, 1993; Andrew and MacVicar, 1994). Integrative optical imaging is used to measure the *ADC*s of molecules tagged with fluorescent dye (Nicholson and Tao, 1993). Diffusion-weighted NMR methods provide information about the water diffusion coefficient (Benveniste et al., 1992; Latour et al., 1994; Norris et al., 1994; Van der Toorn et al., 1996) and as they are non-invasive techniques can be applied to clinical studies. It has been shown that the correlation between water diffusion maps and changes in cell volume and ECS diffusion parameters can be very good (Van der Toorn et al., 1996).

Recordings of IOS, either by light transmittance

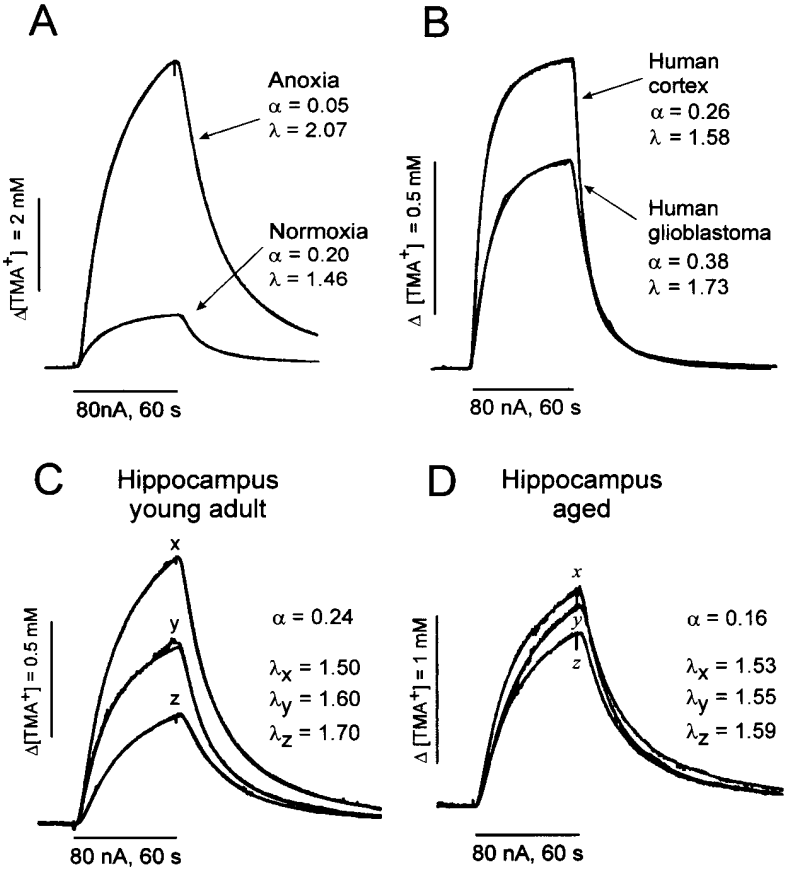

Fig. 6. TMA^+ diffusion curves under different experimental conditions. For each curve, the ECS diffusion parameters α (volume fraction) and λ (tortuosity) were extracted by appropriate non-linear curve fitting. Experimental and theoretical curves are superimposed in each case. For each figure, the concentration scale is linear. (A) Typical diffusion curves obtained in adult rat cortex in vivo (lamina V) during normoxia and in the same animal 10 min after cardiac arrest (Anoxia). Note the decrease in α and increase in λ during anoxia. (B) Typical diffusion curve recorded in a slice (400 μm) from the human temporobasal cortex of an 18-year-old woman with pharmacoresistant epilepsy (Human cortex) and in a slice (400 μm) from a human glioblastoma (grade 4, WHO classification). Note that values of α and λ in glioblastoma are increased, the larger the curve, the smaller the value of α and the slower rise and decay indicate higher tortuosity. (C,D) Diffusion parameters in the hippocampus dentate gyrus of a young adult (C) and an aged rat (D). Note the anisotropic diffusion in the dentate gyrus of a young adult rat. TMA^+ diffusion curves (concentration–time profiles) were measured along three orthogonal axes (x, mediolateral; y, rostrocaudal; z, dorsoventral). The slower rise in the z than in the y direction and in the y than in the x direction indicates a higher tortuosity and more restricted diffusion. The amplitude of the curves shows that TMA^+ concentration is higher along the x-axis than along the y- and z-axes (λ_x, λ_y, λ_z). Actual ECS volume fraction α is about 0.2. (D) In an aged rat, diffusion curves are higher, showing that α is smaller and anisotropy is almost lost.

or by light reflectance, are believed to reflect changes in the ECS volume. However, it recently became evident that under a number of experimental conditions no correlation exists between the IOS and TMA methods (Jarvis et al., 1999; Vargová et al., 1999; Syková et al., 2000). We found that changes in the ECS volume in brain slices measured by the TMA method have a different time course than those revealed by IOS (Fig. 7). Simultaneous measurements using IOS and the TMA method were used to determine the absolute values of the ECS volume fraction, tortuosity and non-specific uptake k' in the dorsal horns of rat spinal cord slices (Vargová et al., 1999; Syková et al., 2000). Cellular swelling, evoked by a 45-min exposure to either 50 mM K^+, hypotonic solution (HS, 160 mOsm kg^{-1}), or NMDA

(10^{-4} and 10^{-3} M), led to a decrease in α and an increase in λ. Within the first 15 min of HS, 50 mM K^+ or NMDA application, the IOS increase reached its peak, but then returned towards control values or even decreased below them. However, the decrease in α of 50–85% and the increase in λ were slower and once the maximum value was reached they remained unchanged for 45 min (Fig. 7). The NMDA-evoked increase in IOS matched the activity-related increase in $[K^+]_e$ (Fig. 7). In comparison with the generalized IOS changes induced by HS or 50 mM K^+, NMDA-evoked changes were distinctly laminar. Changes of IOS and $[K^+]_e$ evoked by NMDA were blocked by Mg^{2+}, but persisted in Ca^{2+}-free solution, Cl^--free solution and after application of furosemide. In contrast, the changes in α and λ diminished in Cl^--free and furosemide solutions. These data suggest that neuronal activity is an important source of IOS changes. It is unlikely that neuronal and glial swelling is the major source of IOS changes as the time course of the α and λ changes are different. It remains to be shown which changes relating to increased neural activity, i.e. changes of cell structure, membrane properties, enzyme activity, ionic movements or pH changes, contribute to IOS. However, there is no doubt that cellular swelling, particularly glial swelling, is responsible for changes in ECS volume and tortuosity, thereby affecting ECS diffusion parameters.

Astrocytic swelling: main cause of ECS volume decrease

The brain has a fixed volume, because it is encased in a rigid skull. Cell swelling, referred to as cytotoxic or cellular edema, occurs simply by a shift of fluid from the extracellular to the intracellular compartment, with a concomitant decrease in the ECS volume (ECS shrinkage), but without an increase in total brain volume. Morphological observations of gray matter have revealed that astrocytic swelling is the primary source of cell swelling (for review see Kimelberg, 2000), although other CNS components also swell. The swelling of astrocytes usually reaches a maximum within 60 min of a pathological insult, such as CNS injury, while fast swelling occurs in a particular region of the neuronal processes. A day or more later, neurons show characteristic degenerative morphological changes which are associated with the appearance of perineuronal swollen astrocytes and delayed cell death (apoptosis) (Kimelberg, 2000).

Questions arise concerning the consequences of cell swelling and ECS volume decrease. Cell swelling, as will be discussed later in this chapter, may result in a decrease of the ECS volume from about 20 to 5% during severe pathologies, e.g. ischemia (Syková et al., 1994; Voříšek and Syková, 1997b). This will result in an increased concentration of neuroactive substances in the ECS, a reduction in the diffusion rate of ions and transmitters in the ECS and have a profound effect on volume transmission, excitability, clearance and the availability of substances in the ECS (Syková, 1997). It has been shown that astrocytic swelling significantly increases intercapillary distance. This may cause a decrease in the capillary lumen and in the diffusion of oxygen to neurons (Garcia, 1997; Auen et al., 1979). Astrocytic swelling also quantitatively affects their intrinsic properties as described in primary astrocyte cultures (Kimelberg and Frangakis, 1985; Pasantes-Morales and Schousboe, 1988). Swollen astrocytes in hypoosmotic media show regulatory volume decrease (RVD), re-establishing their normal volume by losing intracellular ions and amino acids. The loss of excitatory amino acids (e.g. glutamate) could also occur in vivo, activate the receptors on neurons, lead to influx of Ca^{2+} and in high concentrations lead to neuronal death. In vivo, cell swelling is more likely to occur due to a rise in extracellular potassium, e.g. during ischemia, epileptic activity, trauma and excessive stimulation of the afferent input (see below). Mechanistically, astrocytic swelling appears to be a complex phenomenon. Besides exposure to hypoosmotic medium, it may occur by simultaneous operation of Cl^-/HCO_3^- and Na^+/H^+ transporters, extracellular acidosis, an extracellular rise in K^+ leading to the uptake of KCl, net uptake of glutamate and Na^+ or the accumulation of free radicals leading to lipid peroxidation and the breakdown of unsaturated fatty acids (for review see Kimelberg, 2000).

Diffusion barriers formed by glial processes and extracellular matrix

Fine cellular processes produce diffusion barriers and anisotropy. Glial cells when hypertrophied

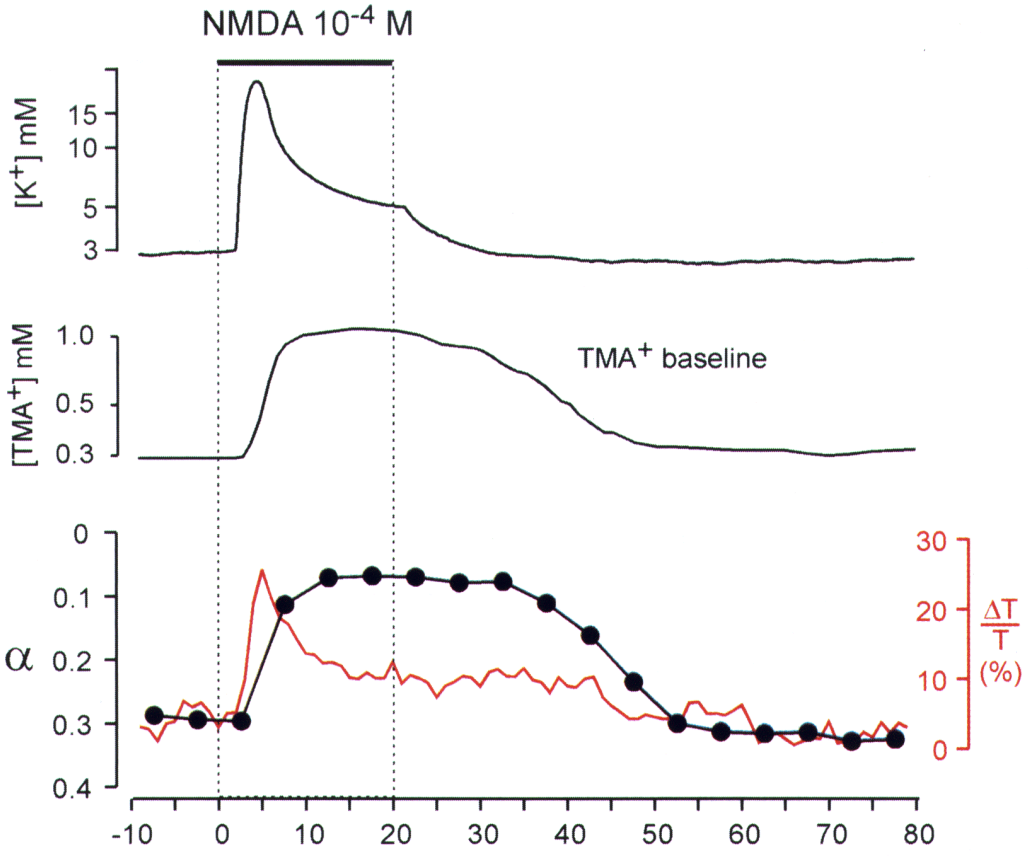
NMDA 10-4 M
[K+] mM
15
10
5
3
[TMA+] mM
1.0
0.5
0.3
TMA+ baseline
α
0
0.1
0.2
0.3
0.4
30
20
10
0
ΔT/T (%)
-10
0
10
20
30
40
50
60
70
80

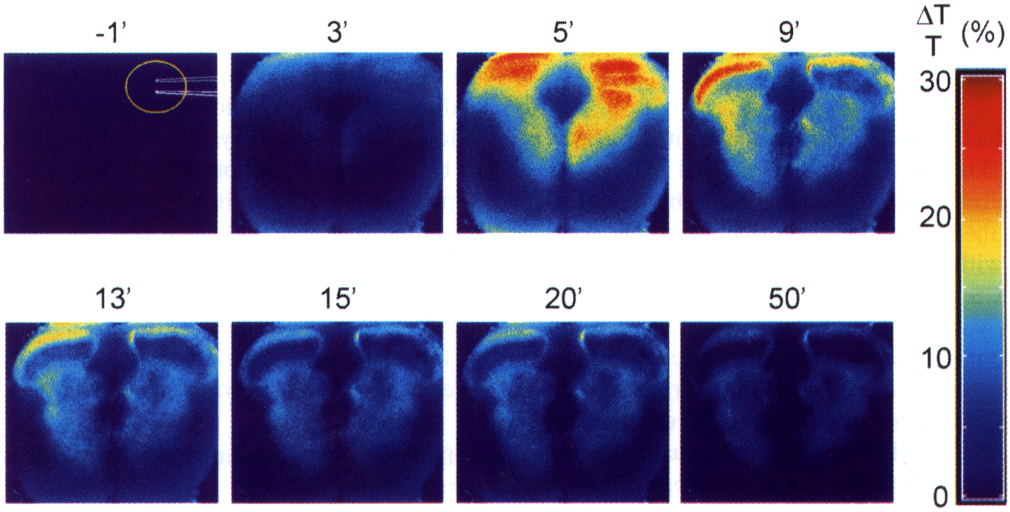
-1'
3'
5'
9'
13'
15'
20'
50'
ΔT/T (%)
30
20
10
0

or proliferating form additional diffusion barriers (Syková, 1997; Roitbak and Syková, 1999) and in this way critically affect the permissiveness of the tissue, synaptic as well as volume transmission, activity-dependent synaptic plasticity, neurogenesis and regeneration.

The solution in the ECS is not a simple salt solution. It has become apparent that long chain polyelectrolytes, either attached or unattached to cellular membranes, are present in the ECS. The ECS also contains a number of glycosaminoglycans (e.g. hyaluronate), glycoproteins and proteoglycans that constitute the extracellular matrix (ECM). The molecular content of the ECM, e.g. chondroitin sulfate proteoglycan, fibronectin, tenascin, laminin, etc. (Thomas and Steindler, 1995; Celio et al., 1998), dynamically changes during development, aging, wound healing and many other pathological processes. ECM molecules are produced by both neurons and glia. These molecules have been suggested to cordon off distinct functional units in the CNS (groups of neurons, axon tracts, and nuclear groups). As shown in Figs. 1 and 4, these large molecules can slow the movement (diffusion) of various neuroactive substances through the ECS. More importantly, these molecules can hinder diffusion of molecules so that they are confined to certain places, while diffusion to other brain regions will be facilitated.

ECM molecules and other large molecules can also affect the tortuosity of the ECS. Their possible effect on changes in TMA^+ diffusion parameters has been studied in rat cortical slices (Tao et al., 1995; Tao and Nicholson, 1996; Vargová et al., 1998) and in isolated rat spinal cord (Prokopová et al., 1996). Superfusion of the slice or spinal cord with a solution containing either 40- or 70-kDa dextran or hyaluronic acid (HA) results in a significant increase in λ. In a standard physiological solution, λ is about 1.57, while in a 1% or 2% solution of 40- or 70-kDa dextran, λ increases to about 1.72–1.77. Application of a 0.1% solution of HA (1.6×10^6 Da) results in an increase in λ to about 2.0. The α is either unchanged or it decreases by less than 10%, suggesting that these substances have no or minimal effect on cell volume and the viability of the preparation.

Modification of the extracellular matrix can also be achieved by enzymatic treatment. Chondroitin sulfate proteoglycans are essential components of the extracellular matrix, forming so-called 'perineuronal nets' surrounding neurons in the cortex and hippocampus. There is also increasing evidence that N-CAM, the protein backbone of polysialic acid (PSA), is involved in synaptic plasticity. PSA, which is almost exclusively carried by N-CAM, is a major modulator of cell adhesion and is high in areas of continuous neurogenesis, neuronal migration, neurite extension and synapse formation. It has been found that mice treated with chondroitinase ABC or with antibodies against N-CAM and transgenic mice lacking the N-CAM gene have impaired long-term potentiation (LTP) (Becker et al., 1996; Muller et al., 1996). It has also been demonstrated that hydrated PSA influences a sufficiently large volume at the cell surface to exert broad steric effects, and that the removal of PSA causes a detectable change in the intercellular space. By contrast, chondroitin sulfate has been found to have little influence on the intercellular space (Yang et al., 1992).

We therefore used a single intracortical injection of endoneuroaminidase NE (endo-N, 10 IU, 5 μU) or chondroitinase ABC (10 μU) and studied the acute (3 h) and chronic (24 h) effects of this treatment on ECS diffusion parameters. A significant decrease in tortuosity is already found in the ipsilateral hemisphere 2 h after injection and persists at 24 h (Mazel and Syková, unpublished data). There is also a small,

Fig. 7. Simultaneous measurements of extracellular potassium concentration ($[K^+]$), the TMA^+ diffusion parameters and light transmittance in spinal cord slices (400 μm) of a 14-day-old rat. Changes in α (ECS volume fraction) before, during and after perfusion of the slice with NMDA (10^{-4}) were extracted by an appropriate non-linear diffusion curve fitting and plotted with the same time course as the light transmittance changes (IOS). Below: IOS images taken 1 min before application ($-1'$; control), and at 3, 5, 9, 13, 15, 20 and 50 min after application of NMDA for 20 min. Cellular, particularly glial, swelling results in an ECS volume decrease. While the changes in TMA diffusion parameters persist during the application period and after the procedure, the changes in IOS decrease with time. It is also evident that the time course of the IOS signal peaks faster than the changes in ECS volume. The changes in IOS, however, correspond to the increase in extracellular $[K^+]$ which corresponds to an increase in neuronal activity. There is, therefore, good correlation of IOS with neuronal excitation, while no simple correlation exists between the IOS signal and ECS volume changes.

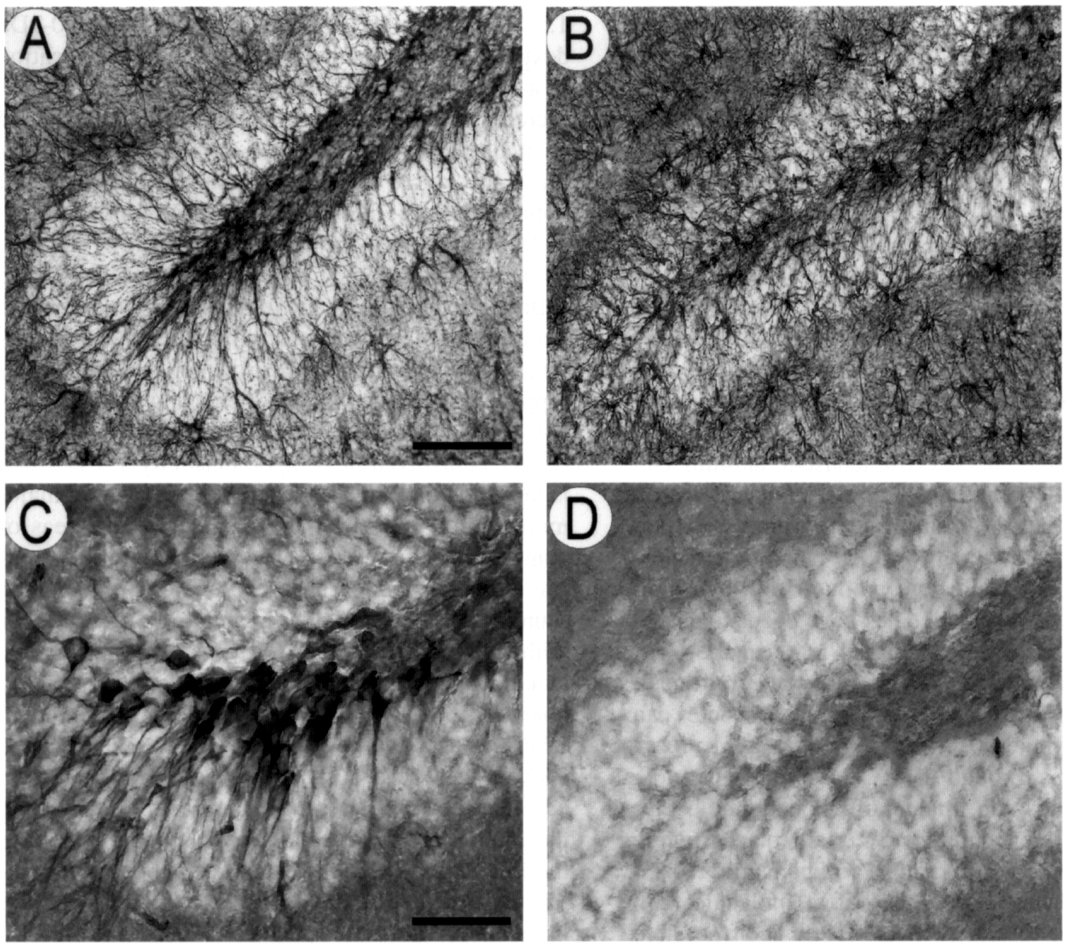

Fig. 8. Structural changes in the hippocampus gyrus dentatus region of aged rats. (A) Astrocytes stained for GFAP in a young adult rat; note the radial organization of the astrocytic processes between the pyramidal cells (not stained). (B) In an aged rat, the radial organization of the astrocytic processes is lost. (C) Staining for fibronectin in a young adult rat shows densely stained cells, apparently due to perineuronal staining around granular cells. (D) In an aged rat, the fibronectin staining is lost. Scale bar: A and B, 100 μm; C and D, 50 μm.

but significant, increase in the ECS volume fraction in the first 3 h after injection that is not found at 24 h.

A decrease in tortuosity and a loss of anisotropy that might be attributed to changes in the ECM have also been found during aging (see below). This decrease correlates with the disappearance of fibronectin and chondroitin sulfate proteoglycans, forming perineuronal nets around granular and pyramidal cells in the hippocampus of young adult rats (Fig. 8). These results suggest that bigger molecules such as 40- and 70-kDa dextran, hyaluronic acid and molecules of the extracellular matrix may slow the diffusion of small molecules, such as TMA^+ (74 Da), ions, neurotransmitters, metabolites etc. in the ECS.

Diffusion inhomogeneity and anisotropy

ECS diffusion parameters are not homogeneous in different parts of the CNS. For example, it has been recognized that the TMA^+ diffusion parameters in the sensorimotor cortex of adult rat in vivo are heterogeneous (Lehmenkühler et al., 1993). The mean volume fraction gradually increases from $\alpha = 0.19$ in cortical layer II to $\alpha = 0.23$ in cortical layer

VI. In subcortical white matter (corpus callosum), the volume fraction is always lower than in cortical layer VI, often between 0.19 and 0.20 (Vořišek and Syková, 1997a; Mazel et al., 1998). There is also a heterogeneity in the spinal cord, the mean values of the volume fraction being highest in the ventral horn and lowest in the white matter (Syková et al., 1994; Šimonová et al., 1996; Prokopová et al., 1997). Similar α values ($\alpha = 0.21$–0.22) have been found throughout the rat brain. In slices from human cortex (temporal and frontal lobe), recently obtained α values were not significantly different, they ranged from 0.21 to 0.26 (Fig. 6).

By introducing the tortuosity factor into diffusion measurements in the CNS, it soon becomes evident that diffusion is not uniform in all directions and that it is affected by diffusion barriers. This so-called anisotropic diffusion preferentially channels the movement of neuroactive substances in the ECS in one direction (e.g. along myelinated axons) and may, therefore, be responsible for a certain degree of specificity in volume transmission. Significant differences in tortuosity have been found in various brain regions, indicating that the local architecture is significantly different. There is increasing evidence that diffusion in brain tissue is anisotropic. Isotropy is defined as the state of constant λ in any direction from a point source, while anisotropy indicates a difference in λ along different axes. To test for anisotropy, the ECS diffusion parameters are measured in three orthogonal axes x, y and z. Indeed, anisotropic diffusion was described using the TMA^+-method in the myelinated white matter of the corpus callosum (Fig. 5), in the spinal cord (Prokopová et al., 1997; Vořišek and Syková, 1997a), in the gray matter of the molecular layer of the cerebellum (Rice et al., 1993), in the hippocampus (Fig. 6C) (Mazel et al., 1998) and in the auditory, but not in the somatosensory, cortex (Syková et al., 1999a). Using MRI, evidence of anisotropic diffusion was also found in the myelinated white matter of cat brain (Moseley et al., 1990) and human brain (Le Bihan et al., 1993). Therefore, not only the diffusion of molecules such as TMA^+ or dextrans, but even the diffusion of water, is prevented by various cellular structures including myelin sheaths. Because of the distinct diffusion characteristics, the extracellular molecular traffic will be different in various brain regions. The anisotropy of myelinated white matter and of gray matter could enable different modes of diffusion transmission in these regions.

Extracellular space diffusion parameters during development

Compared to healthy adults, ECS diffusion parameters significantly differ during postnatal development (Lehmenkühler et al., 1993; Prokopová et al., 1997; Vořišek and Syková, 1997a,b). The ECS volume in the cortex is about twice as large ($\alpha = 0.36$–0.46) in the newborn rat as in the adult rat ($\alpha = 0.21$–0.23), while the tortuosity increases with age. The reduction in the ECS volume fraction correlates well with the growth of blood vessels. The larger ECS in the first days of postnatal development can be attributed to incomplete neuronal migration, gliogenesis and angiogenesis and to the presence of large extracellular matrix proteoglycans, particularly hyaluronic acid, which, due to the mutual repulsion of its highly negatively charged branches, occupies a great deal of space and holds cells apart. In rat spinal cord gray matter, α decreases with neuronal development and gliogenesis from postnatal days 4 to 12 by about 15%, while λ significantly increases, indicating that the diffusion of molecules becomes more hindered with age. The large ECS channels during development may allow the migration of larger substances (e.g. growth factors) and provide better conditions for cell migration during development. On the other hand, the large ECS in the neonatal brain could significantly dilute ions, metabolites and neuroactive substances released from cells, relative to release in adults (Fig. 2), and may be a factor in the prevention of anoxic injury, seizure and spreading depression in young individuals. The diffusion parameters could also play an important role in the developmental process itself. Diffusion parameters are substantially different in myelinated and unmyelinated white matter (Prokopová et al., 1997; Vořišek and Syková, 1997a). Isotropic diffusion is found in the corpus callosum and spinal cord white matter of young rats with incomplete myelination. In myelinated spinal cord and corpus callosum, the tortuosity is higher (the apparent diffusion coefficient is lower) when TMA^+ diffuses across the axons than when it diffuses along the fibers (Fig. 5).

Diffusion properties of the nervous tissue after neonatal X-irradiation

The CNS during the early postnatal period is more sensitive to X-irradiation than the adult nervous system, apparently due to the proliferative potential and increased radiation sensitivity of glial and vascular endothelial cells in the immature nervous system. In experiments on the somatosensory neocortex and subcortical white matter of 1-day-old (P1) rats, X-irradiation at a single dose of 40 Gy results in radiation necrosis with typical early morphological changes in the tissue, namely cell death, DNA fragmentation, extensive neuronal loss, blood–brain barrier (BBB) damage, activated macrophages, astrogliosis, an increase in extracellular fibronectin, and concomitant changes in all three diffusion parameters. The changes are observed as early as 48 h postirradiation and persist at P21 (Syková et al., 1996). Under normal conditions, the volume fraction of the ECS in the cortex is large in newborn rats, $\alpha = 0.35–0.40$, diminishes with age and reaches adult values at P21 (Lehmenkühler et al., 1993). X-irradiation at a single dose of 40 Gy blocks the normal pattern of volume fraction decrease during postnatal development and results in a significant increase in the ECS volume (Syková et al., 1996). The volume fraction in both cortex and corpus callosum increases to about 0.50. This increase persists 3 weeks after X-irradiation. Tortuosity and non-specific uptake significantly decrease at 48 h (P2); at P8–P9, they are not significantly different from those of control animals, and both significantly increase with astrogliosis at P10–P21. These data indicate that in chronic lesions, the volume fraction is elevated, while tortuosity increases due to astrogliosis. Even when X-irradiation at a single dose of 20 Gy is used, resulting in relatively light neuronal damage and loss and BBB damage, it produces similar changes in diffusion parameters as those found with 40 Gy.

Activity-related ECS volume and geometry changes

Transmembrane ionic fluxes during neuronal activity are accompanied by the movement of water and cellular swelling, particularly glial swelling. Changes in ECS diffusion parameters (ECS volume decrease, tortuosity increase and *ADC* decrease) are a consequence of activity-related transmembrane ionic shifts and cellular swelling (Fig. 2). In the spinal cord of the rat or frog, repetitive electrical stimulation results in an ECS volume decrease from about 0.24 to 0.12–0.17, i.e. the ECS volume decreases by as much as 30–50% (Syková, 1987; Svoboda and Syková, 1991). The ECS volume in the spinal dorsal horn of the rat also decreases by 20–50% after injury of the ipsilateral hind paw evoked by subcutaneous injection of turpentine or after thermal injury. The changes in ECS diffusion parameters persist for many minutes after stimulation has ceased (30 min after electrical stimulation or even 120 min after peripheral injury), suggesting long-term changes in neuronal excitability, neuron–glia communication and volume transmission.

To study the role of glia, ECS diffusion parameters were studied in isolated frog filum terminale (FT), which is predominantly composed of glial cells and axons. We studied the cell swelling induced by K^+ application, hypotonic stress and tetanic stimulation of afferent input. Histological analysis revealed that in the central region of the FT, the cell density was lower than in spinal cord, neurons and oligodendrocytes were scarce, glial fibrillary acidic protein (GFAP)-positive astrocytes were abundant, and there were thicker and more densely stained processes than in spinal cord. In the FT, α was 58% higher and λ significantly lower than in the spinal cord. In 50 mM K^+, α in spinal cord decreased from about 0.19 to 0.09, i.e. by 53%, while in FT from about 0.32 to 0.20, i.e. by only 38%. However, λ increased significantly more in FT than in spinal cord. Hypotonic solution resulted in similar decreases in α, and there were no changes in λ in either spinal cord or FT. Stimulation of VIII or IX dorsal root (DR) by 30 Hz evoked an increase in $[K^+]_e$ from 3 to 11–12 mM in spinal cord, but to only 4–5 mM in FT. In the spinal cord, this stimulation led to a 30% decrease in α and a small increase in λ, while in the FT, the decrease in α was only about 10% and there was no increase in λ. It is therefore evident that in the spinal cord — a tissue with a higher density of cellular elements than the FT — 50 mM K^+, hypotonic stress as well as DR stimulation evoked a greater decrease in ECS volume than in FT. Nevertheless, the K^+-induced

increase in tortuosity was higher in FT, suggesting that a substantial part of the K^+-evoked increase in λ was due to astrocytic swelling.

Diffusion barriers after injury and in pathological states

It was shown in a number of studies that astrocyte swelling is an early event in numerous pathological states, accompanied by an elevation of $[K^+]_e$ (Kimelberg and Ransom, 1986; Kimelberg, 1991; Kimelberg et al., 1992). In the isolated turtle cerebellum exposed to hypotonic medium, volume fraction decreased to 0.12, while in hypertonic medium, it increased to as much as 0.60 (Križaj et al., 1996). Cell swelling and astrogliosis (manifested as an increase in GFAP) were also evoked in isolated rat spinal cords by incubation with either 50 mM K^+ or hypotonic solution (235 mOsm kg^{-1}). Application of K^+ or hypotonic solution resulted at first in a decrease in the ECS volume fraction and in an increase in tortuosity in spinal gray matter (Fig. 3D). These changes resulted from cell swelling, since the total water content (TW) in the spinal cord was unchanged and the changes were blocked in Cl^--free solution and slowed down by furosemide and bumetanide. During a continuous 45-min application, α and λ often start returning towards control values, apparently due to the shrinkage of previously swollen cells since TW remains unchanged. This return is blocked by the gliotoxin fluoroacetate, suggesting that most of the changes are due to the swelling of glia. A 45-min application of 50 mM K^+ and, to a lesser degree, of hypotonic solution evokes astrogliosis, which persists after washing out these solutions with physiological saline. During astrogliosis, λ increases again to values as high as 2.0 (Fig. 3D), while α either returns to or increases above control values. This persistent increase in λ after washout is also found in white matter. These data indicate that glial swelling and astrogliosis are associated with a persistent increase in ECS diffusion barriers.

Effects of glutamate, NMDA and AMPA on ECS diffusion parameters, extracellular potassium concentration ($[K^+]_e$) and extracellular pH (pH_e) were studied in the rat isolated spinal cord (Jendelová et al., 2000). Glutamate (10 mM), NMDA (0.1 mM) and AMPA (0.001 mM) evoked a decrease in α by 21, 33 and 21%, respectively, with no substantial effect on λ. These concentrations led to an increase in $[K^+]_e$ of about 5–7 mM and to an initial alkaline shift in pH_e, followed by an acid shift of 0.06–0.08 pH units. Application of higher concentrations of glutamate (10 mM), NMDA (0.1 mM) and AMPA (0.01 mM) evoked decreases in α of 50, 63 and 46%, respectively (Fig. 7). These applications evoked significant increases in λ, $[K^+]_e$ increased to 20–30 mM K^+ (Fig. 7) which was accompanied by a large acid shift of about 0.1–0.2 pH units. The effects of NMDA and AMPA on α, λ, $[K^+]_e$ and pH_e were blocked in Ca^{2+}-free solution and by application of specific antagonists, MK801 and CNQX. The cell swelling induced by excitatory amino acids may therefore result in significant changes in ECS diffusion parameters.

Diffusion barriers during astrogliosis in injured and grafted tissue

Many pathological processes in the central nervous system are accompanied by a loss of cells or neuronal processes, astrogliosis, demyelination, and changes in the extracellular matrix, all of which may affect the apparent diffusion coefficients of neuroactive substances. Several animal models have been developed to study changes in ECS diffusion parameters. Brain injury of any kind elicits reactive gliosis, involving both hyperplasia and hypertrophy of astrocytes, which show intense staining for GFAP (Norton et al., 1992). Astrogliosis is also a typical characteristic of cortical stab wounds in rodents (Norton et al., 1992). The lesion is typically accompanied by an ECS volume increase and a substantial tortuosity increase to mean values of α of about 0.26 and λ of about 1.77 (Roitbak and Syková, 1999).

A stab wound of the rodent brain is a well-characterized and common model of reactive gliosis, which can impose diffusion barriers in the CNS due to the hypertrophy of astrocytic processes and increased production of extracellular matrix components (Hatten et al., 1991; Norton et al., 1992; Ridet et al., 1997). We compared two different methods for revealing diffusion changes in rat cortex after injury: the TMA method and diffusion-weighted MR (Fig. 9). The TMA and MR measurements were performed in the cortex of adult rats from the 3rd to

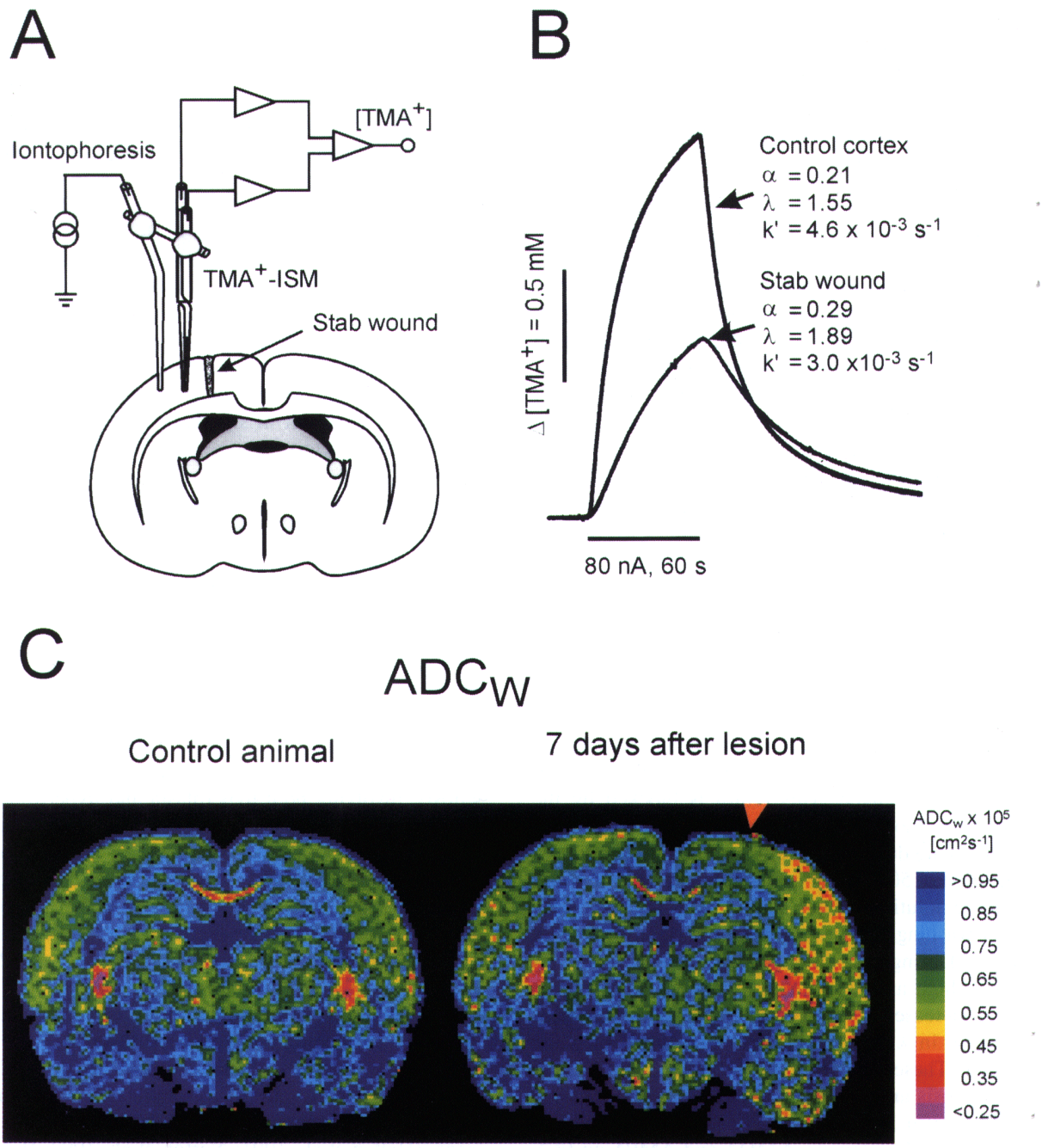

Fig. 9. ECS volume fraction (α), tortuosity (λ) and apparent diffusion coefficient of water (ADC_W) as measured by the TMA method and diffusion-weighted NMR. (A) Experimental setup for TMA diffusion measurements. (B) The ECS volume fraction and tortuosity as measured by the TMA method revealed a significant increase 7 days after the cortical stab wound. α increased only in the vicinity of the wound (up to 1000 μm from the wound), while tortuosity was increased in the whole ipsilateral hemisphere. (C) Pseudocolor images show ADC_W maps of rat brain in a control animal and 7 days after a cortical stab wound. Significant decreases in ADC_W were found in the entire ipsilateral hemisphere including the auditory cortex. This corresponded to an increase in chondroitin sulfate immunostaining (not shown).

the 35th day after a unilateral sterile cut through the cortex. Severe astrogliosis is found close to the injury site (up to 1 mm), and mild astrogliosis up to 2 mm from the wound in the ipsilateral cortex, but no astrogliosis is found in the auditory cortex or in the contralateral hemisphere. In contrast to GFAP staining, immunostaining for chondroitin-sulfate proteoglycan increases in the whole ipsilateral hemisphere (Voříšek et al., 1999; Syková et al., 1999c). The mean values of α, ADC_{TMA} and ADC_W in the contralateral hemisphere were not significantly different from those in non-lesioned, control animals. In the astrogliotic cortex, less than 1 mm distant from the wound, the mean values of α are significantly higher ($\alpha = 0.26$), while the mean values of ADC_{TMA} are lower: (0.42×10^{-5} cm^2 s^{-1}). The more distant from the wound, the less the values of α and ADC_{TMA} differ from control values. On the other hand, ADC_W is significantly lower in the whole ipsilateral hemisphere, particularly in the auditory cortex: $ADC_W = (0.55 \times 10^{-5}$ cm^2 s^{-1}) (Fig. 9). We conclude that an increase in diffusion barriers, manifested by the decrease of both ADC_{TMA} and ADC_W, occurs throughout the entire cortex of the wounded hemisphere without significant changes in ECS volume. The changes are related to astrogliosis, particularly in and closely around the injured area, and to an increase in the extracellular matrix which occurs throughout the entire hemisphere.

These experiments revealed that not only glial swelling and astrogliosis, but also an increase in ECM content, are associated with the long-term increase of diffusion barriers in the ECS, and can, therefore, lead to the impairment of volume transmission and neuroactive substance diffusion (Roitbak and Syková, 1999). Similarly, both the size of the ECS (α) and, surprisingly, λ, are significantly higher in cortical grafts than in host cortex, about 0.35 and 1.79, respectively, this is also the case in gliotic cortex after stab wounds. Both α and λ are increased in cortical grafts of fetal tissue transplanted to the midbrain, where severe astrogliosis compared to host cortex is found, but not in fetal grafts placed into the cavity of the cortex, where only mild astrogliosis occurs (Syková et al., 1999b). Another characteristic feature of cortical grafts into the midbrain is the variability of α and λ. The different values found at various depths of the graft correlate with the morphological heterogeneity of the graft neuropil. These measurements show that even when the ECS in gliotic tissue or in cortical grafts is larger than in normal cortex, the tortuosity is still higher, and the diffusion of chemical signals in such tissue may be hindered. Limited diffusion may also have a negative impact on the viability of grafts in host brains. Compared to host cortex, immunohistochemistry shows myelinated patches and a larger number of hypertrophic astrocytes in areas of high λ values, suggesting that more numerous and/or thicker glial cell processes might be the cause of increased tortuosity.

Extrasynaptic 'volume' transmission of dopamine (DA) plays an important role in Parkinson's disease (PD). The 6-OHDA rat model of PD was used to study how the grafting of fetal DAergic cells affects diffusion of dopamine from a graft into the striatum in vivo (Olshausen et al., 2000). The TMA method allowed measurements of the ECS volume fraction, tortuosity and non-specific uptake. Lesioned rats were divided into three groups; they either received grafts of E14 cell suspensions of ventral midbrain, sham grafts (saline injected) or remained untreated. Age-matched non-lesioned rats served as controls. The cells for intrastriatal transplantation (100,000 in 4 μl) were unilaterally distributed by either two deposits by a metal cannula (macrografts) or eight deposits by a glass capillary (micrografts). The degree of lesion, the survival, function of transplants and the astrogliosis were studied by amphetamine-induced rotational behavior and by immunohistochemistry of tyrosine hydroxylase (TH) and GFAP. We found a functional recovery, good survival of TH-positive cells and astrogliosis in grafted rats 3–5 months after grafting. Prior to diffusion studies grafts were localized by T2 or diffusion-weighted MR, rats were anesthetized and TMA diffusion parameters investigated in the striatum. In non-grafted rats α and λ were unchanged in comparison with controls, while k' decreased. In both grafted and sham grafted rats α increased while k' remained decreased suggesting a lower density of cells in injured tissue. λ increased in the grafts and in the tissue adjacent to them. The increase was significantly large, with macro more pronounced than micrografts. The increase in ECS diffusion barriers corresponded to the astrogliosis in and around the grafts. The increase of extracellular

tortuosity therefore suggests an impediment of DA volume transmission from the grafts (particularly for macrografts) into the lesioned striatum.

Diffusion properties in CNS of GFAP+/+ and GFAP−/− mice

To assess the function of GFAP, the main component of astroglial intermediate filaments, we studied astrocyte membrane properties and the regulation of extracellular space volume in GFAP-negative mice (GFAP−/−). The GFAP gene was disrupted via targeted mutation in embryonic stem cells (Pekny et al., 1995). We compared the ECS diffusion parameters in isolated spinal cord (gray matter) of GFAP−/− and +/+ mice at postnatal days 5, 8 (P5, P8) and in the adult brain (P50–P80). We found no difference in ECS diffusion parameters in GFAP−/− versus +/+ mice at any age or in any brain region. In both groups, λ gradually increases with age to 1.7–1.8 and α decreases to about 0.2 at P50–P80. However, during the application of 50 mM K^+ a significantly greater decrease in volume fraction and increase in tortuosity is seen in GFAP+/+ compared to −/− mice (Fig. 10) (Chvátal et al., 2000). We also found that the wave of spreading depression elicited in the cortex of GFAP+/+ mice by a needle prick is faster than that in GFAP−/− mice, although the final maximal values of the ECS volume fraction decrease and tortuosity increase are not significantly different (Mazel and Syková, 2000).

Using the whole-cell patch-clamp technique, we compared the reversal potential (V_{rev}) of astrocytes and their responses to elevated K^+ and glutamate. Depolarization of GFAP−/− astrocytes in spinal cord slices by 50 mM K^+ is significantly slower than

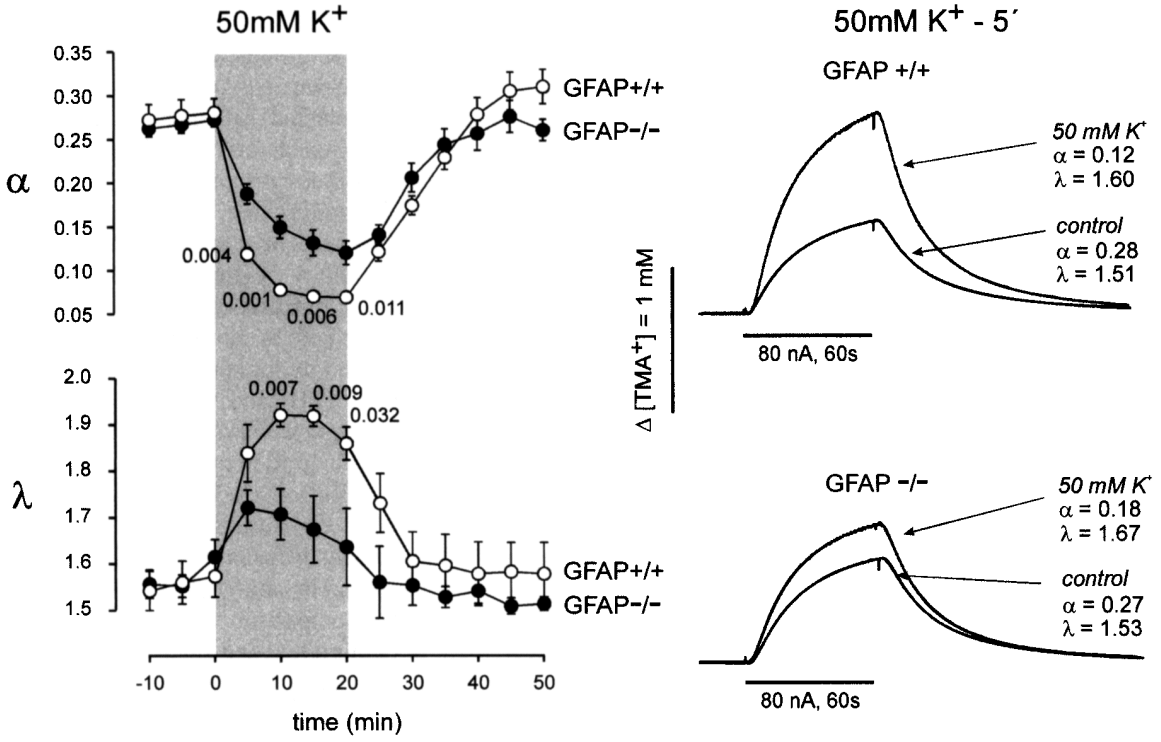

Fig. 10. The effect of 50 mM K^+ on ECS diffusion parameters in the gray matter of mouse spinal cord as measured in GFAP+/+ and GFAP−/− mice (mean ± S.E.M., $n = 4$ in each). Left: each data point represents calculated α and λ values recorded at 5-min intervals. Note that the time course of ECS volume decrease evoked by cell swelling is slower and smaller in GFAP−/− mice and the tortuosity increase is significantly smaller (P values are shown where the difference is significant). Right: typical diffusion curves recorded in the 5 min following 50 mM K^+ application. Note the more rapid decrease in α in GFAP+/+ mice.

that of GFAP+/+ astrocytes. Although the maximal amplitude of the response is not significantly different, its peak is reached later in GFAP−/− astrocytes compared to GFAP+/+ astrocytes. The inward currents evoked by 1 mM glutamate in GFAP−/− astrocytes are smaller and slower than in GFAP+/+ astrocytes by about 40%. In other words, the GFAP−/− astrocytes respond slower to high K^+ and with smaller inward currents to glutamate (Anděrová et al., 1999; Chvátal et al., 2000).

These results suggest that astrocytes in GFAP+/+ and GFAP−/− mice may have different membrane properties, particularly under pathological conditions, e.g. anoxia, ischemia, seizures or repetitive stimulation. GFAP as a structural protein apparently may also affect the ability of astrocytes to change their volume during swelling.

ECS volume and geometry during inflammation and demyelination

Changes in ECS diffusion parameters can be expected during inflammation, during which brain edema may develop. In an experimental model, inflammation was evoked by an intracerebral inoculation of a weakly pathogenic strain of *Staphylococcus aureus* (Lo et al., 1993). Acute inflammation and an increase in BBB permeability in the abscess region resulted in rather mild changes in the ECS diffusion parameters, i.e. the volume fraction tended to be somewhat larger and the tortuosity somewhat smaller.

Dramatic changes in the ECS diffusion parameters are found in the spinal cord of rats during experimental autoimmune encephalomyelitis (EAE), an experimental model of multiple sclerosis (Šimonová et al., 1996). EAE, which is induced by the injection of guinea-pig myelin basic protein (MBP), results in typical morphological changes in the CNS tissue, namely demyelination, an inflammatory reaction, astrogliosis, BBB damage and paraparesis, at 14–17 days post-injection. Paraparesis is accompanied by increases in α in the dorsal horn, in the intermediate region, in the ventral horn and in white matter from about 0.18 to about 0.30. The λ in the dorsal horn and in the intermediate region significantly decreases and k' decreases in the intermediate region and the ventral horn (Šimonová et al., 1996). There is a close correlation between the changes in ECS diffusion parameters and the manifestation of neurological abnormalities.

These results suggest that the expansion of the ECS alters diffusion parameters in inflammatory and demyelinating diseases and may affect the accumulation and movement of ions, neurotransmitters, neuromodulators and metabolites in the CNS in these disorders, possibly by interfering with axonal conduction.

Diffusion properties of gliomas

Cancer is the second leading cause of death in many industrialized countries, and malignant brain tumors, particularly the gliomas, are among the deadliest of tumors, since many patients, including children, die within 2 years. Only recently have basic new findings about tumor cell division, differentiation and migration, the relationship between glial cells and gliomas, the existence of multiple glial precursor cell populations and new insights into the developmental biology of glial cells been made. One of the recently discussed issues is the existence of CNS-specific extracellular matrix proteins, e.g. brain-enriched hyaluronan binding proteins (BEHAB) and brevican, that are expressed at high levels during initial gliogenesis and also in all types and grades of human gliomas (Jaworski et al., 1996). Hyaluronan binding proteins help cells to move through tissue during development and have also been associated with invasive cancers. It has also been suggested that the migration of cells could be critically dependent on their shape and size, their binding to various proteins in the ECS such as hyaluronan-binding protein that may boost the invasiveness of tumors, and on the size and geometry of the ECS. The delivery of drugs to tumors is affected by the permeability of the blood–brain barrier, their diffusion through the ECS in normal and malignant tissue, and their side effects on healthy cells surrounding the tumor. It is therefore crucial to quantify the size, composition and geometry of the extracellular space as these factors critically affect cell migration and the diffusion of substances in the brain (for review see Syková, 1997; Nicholson and Syková, 1998).

Older studies, particularly using sucrose space and electron microscopic methods, have shown that

the visible extracellular compartment is larger in brain tumors, particularly in gliomas, than in normal brain tissue (Bakay, 1970a,b). However, these methods resulted either in small values for the size of the extracellular space because of tissue shrinkage during fixation and embedding, or did not allow one to measure the absolute values of ECS size and geometry or to follow the diffusion of molecules of different sizes and shapes. Increased extracellular space, along with the above-mentioned extracellular matrix proteins, could allow cells to migrate more easily in tumors and into surrounding tissue. Shrinkage of the extracellular space and extracellular matrix proteins could slow or substantially limit the diffusion and migration of cells.

To quantify extracellular space size, geometry and diffusion properties in tumors (particularly malignant gliomas) TMA measurements were performed in slices from surgically removed pieces of patients' brains (Vargová et al., 2000). We found that the more malignant the glioma, the more dramatic the increase in ECS volume. In many brain slices from glioblastomas (grade 4, WHO classification system), the ECS volume is as large as 37–46% of total tissue volume (Fig. 6). There is also an increase in tortuosity which can be due either to the frequently observed astrogliosis or to changes in the extracellular matrix. It is therefore reasonable to assume that the ECS composition, volume and geometry play an important role in cancer malignancy and invasiveness. The size of the ECS in malignant tumors and their geometry and structure could be taken into account during therapeutic drug delivery.

ECS diffusion parameters and aging

In the mammalian brain, higher cognitive functions, such as learning and memory, depend upon the circuits that run through the hippocampus. Until recently, learning deficits during aging have been associated with neuronal degeneration and synaptic inefficiency. However, recent observations of a lack of hippocampal cell loss in aged humans, monkeys and rats (West, 1993; Rapp and Gallagher, 1996; Rasmussen et al., 1996) suggest that age-related functional changes in the nervous system may not necessarily be a sign of degenerative pathology. The question thus arises whether learning deficits during aging and Alzheimer's disease also involve the impairment of extrasynaptic or 'volume' transmission, i.e. the diffusion of neuroactive substances in the ECS.

Aging, Alzheimer's disease and many degenerative diseases are accompanied by various pathological processes including a decreased number and efficacy of synapses, a decrease in transmitter release, neuronal loss, astrogliosis, demyelination, deposits of β-amyloid, changes in extracellular matrix proteins, etc. In a recent study of the rat brain, morphological changes during aging included cell loss, loss of dendritic processes, demyelination, astrogliosis, swollen astrocytic processes and changes in the extracellular matrix. Increased GFAP staining and an increase in the size and fibrous character of astrocytes were found in the cortex, corpus callosum and hippocampus of senescent rats, which may account for changes in the ECS volume fraction (Syková et al., 1998a).

ECS diffusion parameters were measured in the cortex, corpus callosum and hippocampus (CA1, CA3 and dentate gyrus). TMA^+ diffusion was measured in the ECS independently along three orthogonal axes (x, transversal; y, sagittal; z, vertical). In all three regions — cortex, corpus callosum and hippocampus — the mean ECS volume fraction α was significantly lower in aged rats (26–32 months old), ranging from 0.16 to 0.18, than in young adults (3–4 months old) in which α ranged from 0.21 to 0.22 (Fig. 6C,D). Non-specific uptake k' was also significantly lower in aged rats.

Morphological changes other than those accounting for the α decrease could account for decreases in λ values and for the disruption of tissue anisotropy. In the hippocampus in CA1, CA3, as well as in the dentate gyrus, we observed changes in the arrangement of fine astrocytic processes (Fig. 8). These are normally organized in parallel in the x–y plane, this organization totally disappears during aging. Moreover, the decreased staining for chondroitin sulfate proteoglycans and for fibronectin suggests a loss of extracellular matrix macromolecules (Fig. 8). Although the mean tortuosity values along the x-axis were not significantly different between young and aged rats, the values were significantly lower in aged rats along the y- and z-axes, and thus the values along all three axes become almost the same (Fig. 6C,D).

This means that there is a loss of anisotropy in the aging hippocampus, particularly in the CA3 region and the dentate gyrus (Syková et al., 1998a).

What is the functional significance of the observed changes in ECS diffusion parameters during aging? We suggest that the alterations in hippocampal diffusion parameters seen in aged animals with severe learning deficits may account for the learning impairment, either due to their effect on volume transmission (Nicholson and Syková, 1998) or on 'cross-talk' between synapses, which has been suggested to be involved in LTP and LTD (Kullmann et al., 1996), or on both. Anisotropy, which, particularly in the hippocampus and corpus callosum, may help facilitate the diffusion of neurotransmitters and neuromodulators to regions occupied by their high affinity extrasynaptical receptors, might have crucial importance for the specificity of signal transmission. The importance of anisotropy for the 'spill-over of glutamate', 'cross-talk' between synapses, and for LTP and LTD has been proposed (Kullmann et al., 1996; Asztely et al., 1997). The observed loss of anisotropy in senescent rats could therefore lead to impaired cortical and, particularly, hippocampal function. The decrease in ECS size could be responsible for the greater susceptibility of the aged brain to pathological events, such as ischemia, cell death during anesthesia (Syková et al., 1998a,b), the poorer outcome of clinical therapy and the more limited recovery of affected tissue after insult.

Are glial membrane properties affected by regional differences in ECS volume?

It was shown in recent studies that the regional differences in extracellular space volume around glial cells in the CNS affect their membrane currents in response to voltage steps (Berger et al., 1991; Chvátal et al., 1997, 1999). In experiments performed in the gray matter of the spinal cord slice, i.e. in tissue containing neurons as well as mature astrocytes and oligodendrocytes and their respective precursors (Chvátal et al., 1995), the occurrence of large tail currents was observed only in oligodendrocytes but not in other cell types (Chvátal et al., 1999). As calculated from the Nernst equation, changes in the reversal potentials of the tail currents revealed a significantly larger accumulation of $[K^+]_e$ around oligodendrocytes than around astrocytes during the depolarization of the cells, apparently due to the more 'compact' ECS around oligodendrocytes. The application of 50 mM K^+ or hypotonic solution, used to study the effects of cell swelling on $[K^+]_e$ changes evoked by a depolarizing pulse, produced in the vicinity of astrocytes an increase in $[K^+]_e$ in the range of 200–240%, while in oligodendrocytes, the increase was only 22–30%.

ECS diffusion measurements in nervous tissue, which are performed by means of the real-time iontophoretic method over a volume on the order of 10^{-3} mm^3, do not provide information about the properties of the ECS in the vicinity of individual nerve cells. Nevertheless, using tail current analysis to study the glial membrane properties it became evident that the larger K^+ accumulation in the vicinity of the oligodendrocyte membrane results from a smaller ECS volume around oligodendrocytes than around astrocytes. These results also indicate that the swelling is more pronounced in astrocytes than in oligodendrocytes, and it is possible to speculate that astrocytes are responsible for the majority of the cell volume changes in nervous tissue. In addition, the electrophysiological properties of oligodendrocytes, i.e., the K^+ influx indicated by the presence of tail currents, show that this type of cell may efficiently contribute to the regulation of K^+ changes arising from neuronal activity.

Conclusions and summary

In conclusion, glial cells control not only ECS ionic composition, but also ECS size and geometry. Since ECS ionic and volume changes have been shown to play an important role in modulating the complex synaptic and extrasynaptic signal transmission in the CNS, glial cells may thus affect neuronal interaction, synchronization and neuron–glia communication. As shown in Fig. 2, a link between ionic and volume changes and signal transmission has been proposed as a model for the non-specific feedback mechanism suppressing neuronal activity (Syková, 1997; Ransom, 2000). First, neuronal activity results in the accumulation of $[K^+]_e$, which in turn depolarizes glial cells, and this depolarization induces an alkaline shift in glial pH_i. Second, the glial cells extrude acid and the resulting acid shift causes a decrease in the

neuronal excitability. Because ionic transmembrane shifts are always accompanied by water, this feedback mechanism is amplified by activity-related glial swelling compensated for by ECS volume shrinkage and by increased tortuosity, presumably by the crowding of molecules of the ECS matrix and/or by the swelling of fine glial processes. This, in turn, results in a larger accumulation of ions and other neuroactive substances in the brain due to increased diffusion hinderance in the ECS.

Astrocyte hypertrophy, proliferation and swelling influence the size of the ECS volume and tortuosity around neurons, slowing diffusion in the ECS. Their organization may also affect diffusion anisotropy, which could be an underlying mechanism for the specificity of extrasynaptic transmission, including 'cross-talk' between distinct synapses (Barbour and Hausser, 1997; Kullmann and Asztely, 1998). An increased concentration of transmitter released into a synapse (e.g. repetitive adequate stimuli or during high frequency electrical stimulation which induces LTP) results in a significant activation of high-affinity receptors at neighboring synapses. The efficacy of such synaptic cross-talk would be dependent on the extracellular space surrounding the synapses, i.e. on intersynaptic geometry and diffusion parameters. Other recent studies have also suggested an important role for proteoglycans, known to participate in multiple cellular processes, such as axonal outgrowth, axonal branching and synaptogenesis (Hardington and Fosang, 1992; Margolis and Margolis, 1993) that are important for the formation of memory traces. Recent observation of a decrease of fibronectin and chondroitin sulfate proteoglycan staining in the hippocampus of behaviorally impaired aged rats (Syková et al., 1998a,b) supports this hypothesis. It is reasonable to assume that besides neuronal and glial processes, macromolecules of the extracellular matrix contribute to diffusion barriers in the ECS. It is therefore apparent that glial cells play an important role in the local architecture of the CNS and they may also be involved in the modulation of signal transmission, in plastic changes, LTP, LTD and in changes of behavior and memory formation.

Abbreviations

ADC	apparent diffusion coefficient
BBB	blood–brain barrier
BEHAB	brain enriched hyaluronan binding proteins
DA	dopamine
EAE	experimental autoimmune encephalomyelitis
ECS	extracellular space
FT	filum terminale
GABA	γ-aminobutyric acid
GFAP	glial fibrillary acidic protein
IOI	integrative optical imaging
IOS	intrinsic optical signals
ISM	ion-sensitive microelectrodes
LTP	long-term potentiation
MBP	myelin basic protein
N-CAM	neural cell adhesion molecule
NMDA	*N*-methyl-D-aspartate
NMR	nuclear magnetic resonance
P	postnatal day
PD	Parkinson's disease
PSA	polysialic acid
TH	tyrosine hydroxylase
TW	total water content

Acknowledgements

Supported by Grants VS96-130, GACR 307/96/K226, GACR 309/97/K048, GACR 309/99/0657, GACR 305/99/0655 and GACR 309/00/1430.

References

Agnati, L.F., Zoli, M., Stromberg, I. and Fuxe, K. (1995) Intercellular communication in the brain: wiring versus volume transmission. *Neuroscience*, 69: 711–726.

Anděrová, M., Chvátal, A., Eliasson, C., Pěkný, M. and Syková, E. (1999) Membrane properties and swelling of astrocytes in GFAP−/− mice. *Physiol. Res.*, 48: S52.

Andrew, R.D. and MacVicar, B.A. (1994) Imaging cell volume changes and neuronal excitation in the hippocampal slice. *Neuroscience*, 62: 371–383.

Asztely, F., Erdemli, G. and Kullmann, D.M. (1997) Extrasynaptic glutamate spillover in the hippocampus: dependence on temperature and the role of active glutamate uptake. *Neuron*, 18: 281–293.

Auen, E.L., Bourke, R.S. and Barron, K.D. (1979) Alterations in cat cerebrospinal capillary morphometric parameters following K+ induced cerebrocortical swelling. *Acta Neuropathol.*, 47: 175–181.

Bakay, L. (1970a) The extracellular space in brain tumor. I. Morphological considerations. *Brain*, 93: 693–698.

Bakay, L. (1970b) The extracellular space in brain tumor. II. The sucrose space. *Brain*, 93: 699–707.

Barbour, B. and Hausser, M. (1997) Intersynaptic diffusion of neurotransmitter. *Trends Neurosci.*, 20: 377–384.

Becker, C.G., Artola, A., Gerardy-Schahn, R., Becker, T., Welzl, H. and Schachner, M. (1996) The polysialic acid modification of the neural cell adhesion molecule is involved in spatial learning and hippocampal long-term potentiation. *J. Neurosci. Res.*, 45: 143–152.

Benveniste, H., Hedlund, L.W. and Johnson, G.A. (1992) Mechanism of detection of acute cerebral ischemia in rats by diffusion-weighted magnetic resonance microscopy. *Stroke*, 23: 746–754.

Berger, T., Schnitzer, J. and Kettenmann, H. (1991) Developmental changes in the membrane current pattern, K^+ buffer capacity and morphology of glial cells in the corpus callosum slice. *J. Neurosci.*, 11: 3008–3024.

Celio, M.R., Spreafico, R., De Biasi, S. and Vitellaro-Zuccarello, L. (1998) Perineuronal nets: past and present. *Trends Neurosci.*, 21: 510–515.

Chvátal, A., Pastor, A., Mauch, M., Syková, E. and Kettenmann, H. (1995) Distinct populations of identified glial cells in the developing rat spinal cord: ion channel properties and cell morphology. *Eur. J. Neurosci.*, 7: 129–142.

Chvátal, A., Berger, T., Vořišek, I., Orkand, R.K., Kettenmann, H. and Syková, E. (1997) Changes in glial K^+ currents with decreased extracellular volume in developing rat white matter. *J. Neurosci. Res.*, 49: 98–106.

Chvátal, A., Anděrová, M., Žiak, D. and Syková, E. (1999) Glial depolarization evokes a larger potassium accumulation around oligodendrocytes than around astrocytes in gray matter of rat spinal cord slices. *J. Neurosci. Res.*, 56: 493–505.

Chvátal, A., Anděrová, M., Kubinová, Š., Eliasson, C., Pekny, M. and Syková, E. (2000) Swelling and membrane properties of astrocytes in spinal cords of GFAP-deficient mice. *Abstracts, IV European Meeting on Glial Cell Function in Health and Disease*, 79.

Chesler, M. (1990) The regulation and modulation of pH in the nervous system. *Prog. Neurobiol.*, 34: 401–427.

Deitmer, J.W. and Rose, C.R. (1996) pH regulation and proton signaling by glial cells. *Prog. Neurobiol.*, 48: 73–103.

Fuxe, K. and Agnati, L.F. (1991) *Volume Transmission in the Brain: Novel Mechanisms for Neural Transmission*. Raven Press, New York.

Garcia, J.H. (1997) Evolution of the brain lesion induced by experimental focal ischemia. In: K.M.A. Welch, L.R. Caplan, D.J. Reis, B.K. Siesjo and B. Weir (Eds.), *Primer on Cerebrovascular Diseases*. Academic Press, San Diego, pp. 107–111.

Hardington, T.E. and Fosang, A.J. (1992) Proteoglycans: many forms and many functions. *FASEB J.*, 6: 861–870.

Hatten, M.E., Liem, R.K.H., Shelanski, M.L. and Mason, C.A. (1991) Astroglia in CNS injury. *Glia*, 4: 233–243.

Jarvis, C.R., Lilge, L., Vipond, G.J. and Andrew, D. (1999) Interpretation of intrinsic optical signals and calcein fluorescence during acute excitotoxic insult in the hippocampal slice. *Neuroimage*, 10: 357–372.

Jaworski, D.M., Kelly, G.M. and Hockfield, S. (1996) The CNS-specific hyaluronan binding protein, BEHAB, is expressed during periods of glial cell generation and motility. *Semin. Neurosci.*, 8: 391–396.

Jendelová, P. and Syková, E. (1991) Role of glia in K^+ and pH homeostasis in the neonatal rat spinal cord. *Glia*, 4: 56–63.

Jendelová, P., Chvátal, A., Šimonová, Z. and Syková, E. (1994) Effect of excitatory amino acids on extracellular pH in isolated rat spinal cord. In: *Abstracts, 17th Annual Meeting ENA*, Vienna, p. 199.

Jendelová, P., Vargová, L. and Syková, E. (2000) Effect of glutamate on extracellular space diffusion parameters, K^+ and pH in the isolated rat spinal cord. *FENS*, Brighton. *Eur. J. Neurosci.*, 12: 397.

Kimelberg, H.K. (1991) Swelling and volume control in brain astroglial cells. In: R. Gilles (Ed.), *Advances in Comparative and Environmental Physiology*, Springer Verlag, Berlin, pp. 81–117.

Kimelberg, H.C. (2000) Cell volume in the CNS: regulation and implications for nervous system function and pathology. *Neuroscientist*, 6: 13–24.

Kimelberg, H.K. and Frangakis, M.V. (1985) Furosemide- and bumetanide-sensitive ion transport and volume control in primary astrocyte cultures from rat brain. *Brain Res.*, 361: 125–134.

Kimelberg, H.K. and Ransom, B.R. (1986) Physiological and pathological aspects of astrocyte swelling. In: S. Federoff and A. Vernadakis (Eds.), *Astrocytes: Cell Biology and Pathology of Astrocytes*, Academic Press, New York, pp. 129–166.

Kimelberg, H.K., Sankar, P., O'Connor, E.R., Jalonen, T. and Goderie, S.K. (1992) Functional consequences of astrocyte swelling. *Prog. Brain Res.*, 94: 57–68.

Korf, J., Klein, H.C. and Postrema, F. (1988) Increases in striatal and hippocampal impedance and extracellular levels of amino acids by cardiac arrest in freely moving rats. *J. Neurochem.*, 50: 1087–1096.

Križaj, D., Rice, M.E., Wardle, R.A. and Nicholson, C. (1996) Water compartmentalization and extracellular tortuosity after osmotic changes in cerebellum of *Trachemys scripta*. *J. Physiol.*, 492: 887–896.

Kullmann, D.M. and Asztely, F. (1998) Extrasynaptic glutamate spillover in the hippocampus: evidence and implications. *Trends Neurosci.*, 21: 8–14.

Kullmann, D.M., Erdemli, G. and Asztely, F. (1996) LTP of AMPA and NMDA receptor-mediated signals: evidence for presynaptic expression and extrasynaptic glutamate spill-over. *Neuron*, 17: 461–474.

Latour, L.L., Svoboda, K., Mitra, P.P. and Sotak, C.H. (1994) Time-dependent diffusion of water in a biological model system. *Proc. Natl. Acad. Sci. USA*, 91: 1229–1233.

Le Bihan, D., Turner, R. and Douek, P. (1993) Is water diffusion restricted in human brain white matter? An echoplanar NMR imaging study. *NeuroReport*, 4: 887–890.

Lehmenkühler, A., Syková, E., Svoboda, J., Zilles, K. and Nicholson, C. (1993) Extracellular space parameters in the

rat neocortex and subcortical white matter during postnatal development determined by diffusion analysis. *Neuroscience*, 55: 339–351.

Lo, W.D., Wolny, A.C., Timan, C., Shin, D. and Hinkle, G.H. (1993) Blood–brain barrier permeability and the brain extracellular space in acute cerebral inflammation. *J. Neurol. Sci.*, 118: 188–193.

Margolis, R.K. and Margolis, R.U. (1993) Nervous tissue proteoglycans. *Experientia*, 49: 429–446.

Matsuoka, Y. and Hossmann, K.A. (1982) Cortical impedance and extracellular volume changes following middle cerebral artery occlusion in cats. *J. Cereb. Blood Flow Metab.*, 2: 466–474.

Mazel, T. and Syková, E. (2000) Absence of GFAP affects astrocyte swelling and extracellular space diffusion parameters in mouse cortex. *Abstracts, IV European Meeting on Glial Cell Function in Health and Disease*, 94.

Mazel, T., Šimonová, Z. and Syková, E. (1998) Diffusion heterogeneity and anisotropy in rat hippocampus. *NeuroReport*, 9: 1299–1304.

Moseley, M.E., Cohen, Y., Mintorovitch, J., Chileuitt, L., Shimizu, H., Kucharczyk, J., Wendland, M.F. and Weinstein, P.R. (1990) Early detection of regional cerebral ischemia in cats: comparison of diffusion- and T2-weighted MRI and spectroscopy. *Magn. Reson. Med.*, 14: 330–346.

Muller, D., Wang, C., Skibo, G., Toni, N., Cremer, H., Calaora, V., Rougon, G. and Kiss, J.Z. (1996) PSA-NCAM is required for activity-induced synaptic plasticity. *Neuron*, 17: 413–422.

Ng, K.T., Gibbs, M.E., Crowe, S.F., Sedman, G.L., Hua, F., Zhao, W., O'Dowd, B., Rickard, N., Gibbs, C.L., Syková, E., Svoboda, J. and Jendelová, P. (1991) Molecular mechanisms of memory function. *Mol. Neurobiol.*, 5: 333–350.

Nicholson, C. (1995) Interaction between diffusion and Michaelis–Menten uptake of dopamine after iontophoresis in striatum. *Biophys. J.*, 68: 1699–1715.

Nicholson, C. and Phillips, J.M. (1981) Ion diffusion modified by tortuosity and volume fraction in the extracellular microenvironment of the rat cerebellum. *J. Physiol.*, 321: 225–257.

Nicholson, C. and Syková, E. (1998) Extracellular space structure revealed by diffusion analysis. *Trends Neurosci.*, 21: 207–215.

Nicholson, C. and Tao, L. (1993) Hindered diffusion of high molecular weight compounds in brain extracellular microenvironment measured with integrative optical imaging. *Biophys. J.*, 65: 2277–2290.

Norris, D.G., Niendorf, T. and Leibfritz, D. (1994) Healthy and infarcted brain tissues studied at short diffusion times: the origins of apparent restriction and the reduction in apparent diffusion coefficient. *NMR Biomed.*, 7: 304–310.

Norton, W.T., Aquino, D.A., Hosumi, I., Chiu, F.C. and Brosnan, C.F. (1992) Quantitative aspects of reactive gliosis: a review. *Neurochem. Res.*, 17: 877–885.

Olshausen, F., Reum, T., Mazel, T., Voříšek, I., Morgenstern, R. and Syková, E. (2000) Extracellular diffusion in the striatum of 6-OHDA-lesioned and grafted rats. *Soc. Neurosci. Abstr.*, 26: 870.

Pasantes-Morales, H. and Schousboe, A. (1988) Volume regulation in astrocytes: a role for taurine as an osmoeffector. *J. Neurosci. Res.*, 20: 503–509.

Pekny, M., Leveen, P., Pekna, M., Eliasson, C., Berthold, C.H., Westermark, B. and Betsholtz, C. (1995) Mice lacking glial fibrillary acidic protein display astrocytes devoid of intermediate filaments but develop and reproduce normally. *EMBO J.*, 14: 1590–1598.

Prokopová, Š., Nicholson, C. and Syková, E. (1996) The effect of 40-kDa or 70-kDa dextran and hyaluronic acid solution on extracellular space tortuosity in isolated rat spinal cord. *Physiol. Res.*, 45: P28.

Prokopová, Š., Vargová, L. and Syková, E. (1997) Heterogeneous and anisotropic diffusion in the developing rat spinal cord. *NeuroReport*, 8: 3527–3532.

Ransom, B.R. (2000) Glial modulation of neural excitability mediated by extracellular pH: a hypothesis revisited. In: L.F. Agnati, K. Fuxe, C. Nicholson and E. Syková (Eds.), *Volume Transmission Revisited*. Elsevier Science, Amsterdam, pp. 217–229.

Rapp, P.R. and Gallagher, M. (1996) Preserved neuron number in the hippocampus of aged rats with spatial learning deficits. *Proc. Natl. Acad. Sci. USA*, 93: 9926–9930.

Rasmussen, T., Schliemann, T., Sorensen, J.C., Zimmer, J. and West, M.J. (1996) Memory impaired aged rats: no loss of principal hippocampal and subicular neurons. *Neurobiol. Aging*, 17: 143–147.

Rice, M.E., Okada, Y.C. and Nicholson, C. (1993) Anisotropic and heterogeneous diffusion in the turtle cerebellum: implications for volume transmission. *J. Neurophysiol.*, 70: 2035–2044.

Ridet, J.I., Malhotra, S.K., Privat, A. and Gage, F.H. (1997) Reactive astrocytes: cellular and molecular cues to biological function. *Trends Neurosci.*, 20: 570–577.

Roitbak, T. and Syková, E. (1999) Diffusion barriers evoked in the rat cortex by reactive astrogliosis. *Glia*, 20: 40–48.

Šimonová, Z., Svoboda, J., Orkand, R., Bernard, C.C.A., Lassmann, H. and Syková, E. (1996) Changes of extracellular space volume and tortuosity in the spinal cord of Lewis rats with experimental autoimmune encephalomyelitis. *Physiol. Res.*, 45: 11–22.

Svoboda, J. and Syková, E. (1991) Extracellular space volume changes in the rat spinal cord produced by nerve stimulation and peripheral injury. *Brain Res.*, 560: 216–224.

Syková, E. (1983) Extracellular K^+ accumulation in the central nervous system. *Prog. Biophysiol. Mol. Biol.*, 42: 135–189.

Syková, E. (1987) Modulation of spinal cord transmission by changes in extracellular K^+ activity and extracellular volume. *Can. J. Physiol. Pharmacol.*, 65: 1058–1066.

Syková, E. (1992) *Ionic and Volume Changes in the Microenvironment of Nerve and Receptor Cells*. Springer Verlag, Heidelberg.

Syková, E. (1997) The extracellular space in the CNS: its regulation, volume and geometry in normal and pathological neuronal function. *Neuroscientist*, 3: 28–41.

Syková, E., Jendelová, P., Šimonová, Z. and Chvátal, A. (1992) K^+ and pH homeostasis in the developing rat spinal cord is

impaired by early postnatal X-irradiation. *Brain Res.*, 594: 19–30.

Syková, E., Svoboda, J., Polák, J. and Chvátal, A. (1994) Extracellular volume fraction and diffusion characteristics during progressive ischemia and terminal anoxia in the spinal cord of the rat. *J. Cereb. Blood Flow Metab.*, 14: 301–311.

Syková, E., Svoboda, J., Šimonová, Z., Lehmenkühler, A. and Lassmann, H. (1996) X-irradiation-induced changes in the diffusion parameters of the developing rat brain. *Neuroscience*, 70: 597–612.

Syková, E., Mazel, T., Frisch, C., Šimonová, Z., Hasenöhrl, R.U. and Huston, J.P. (1998a) Spatial memory and diffusion parameters in aged rat cortex, corpus callosum and hippocampus. *Soc. Neurosci. Abstr.*, 24: 1420.

Syková, E., Mazel, T. and Šimonová, Z. (1998b) Diffusion constraints and neuron–glia interaction during aging. *Exp. Gerontol.*, 33: 837–851.

Syková, E., Mazel, T., Roitbak, T. and Šimonová, Z. (1999a) Morphological changes and diffusion barriers in auditory cortex and hippocampus of aged rats. *Assoc. Res. Otolaryngol. Abstr.*, 22: 17.

Syková, E., Roitbak, T., Mazel, T., Šimonová, Z. and Harvey, A.R. (1999b) Astrocytes, oligodendroglia, extracellular space volume and geometry in rat fetal brain grafts. *Neuroscience*, 91: 783–798.

Syková, E., Vořišek, I., Tintěra, J., Roitbak, T. and Nicolay, K. (1999c) Water ADC, extracellular space volume and tortuosity in a rat model of injury. *Soc. Neurosci. Abstr.*, 25: 823.

Syková, E., Vargová, L., Jendelová, P. and Chvátal, A. (2000) Intrinsic optical signals evoked in spinal cord slices and their relation to neuronal activity and cell swelling. *Soc. Neurosci. Abstr.*, 26: 1619.

Tao, L. and Nicholson, C. (1996) Diffusion of albumins in rat cortical slices and relevance to volume transmission. *Neuroscience*, 75: 839–847.

Tao, L., Vořišek, I., Lehmenkühler, A., Syková, E. and Nicholson, C. (1995) Comparison of extracellular tortuosity derived from diffusion of 3 kDa dextran and TMA+ in rat cortical slices. *Soc. Neurosci. Abstr.*, 21: 604.

Thomas, L.B. and Steindler, D.A. (1995) Glial boundaries and scars: programs for normal development and wound healing in the brain. *Neuroscientist*, 1: 142–154.

Van der Toorn, A., Syková, E., Dijkhuizen, R.M., Vořišek, I., Vargová, L., Škobisová, E., Van Lookeren Campagne, M., Reese, T. and Nicolay, K. (1996) Dynamic changes in water ADC, energy metabolism, extracellular space volume, and tortuosity in neonatal rat brain during global ischemia. *Magn. Reson. Med.*, 36: 52–60.

Van Harreveld, A., Dafny, N. and Khattab, F.I. (1971) Effects of calcium on electrical resistance and the extracellular space of cerebral cortex. *Exp. Neurol.*, 31: 358–367.

Vargová, L., Tao, L., Syková, E., Ulbrich, K., Šubr, V. and Nicholson, C. (1998) Diffusion of large polymers in rat cortical slices measured by integrative optical imaging. *J. Physiol.*, 511: 16P.

Vargová, L., Prokopová, Š., Chvátal, A. and Syková, E. (1999) Are the changes in intrinsic optical signals a tool to measure changes in extracellular space volume?. *Soc. Neurosci. Abstr.*, 25: 742p.

Vargová, L., Homola, A., Jendelová, P., Zamečník, J., Tichý, M., Beneš, V. and Syková, E. (2000) Extracellular space volume fraction and geometry in human cortex and gliomas. *Soc. Neurosci. Abstr.*, 26: 1619.

Vořišek, I. and Syková, E. (1997a) Evolution of anisotropic diffusion in the developing rat corpus callosum. *J. Neurophysiol.*, 78: 912–919.

Vořišek, I. and Syková, E. (1997b) Ischemia-induced changes in the extracellular space diffusion parameters, K^+ and pH in the developing rat cortex and corpus callosum. *J. Cereb. Blood Flow Metab.*, 17: 191–203.

Vořišek, I., Roitbak, T., Nicolay, K. and Syková, E. (1999) Water ADC, extracellular space volume and tortuosity in the rat cortex during astrogliosis. *Physiol. Res.*, 48: S136.

Walz, W. (1989) Role of glial cells in the regulation of the brain ion microenvironment. *Prog. Neurobiol.*, 33: 309–333.

West, M.J. (1993) Regionally specific loss of neurons in the aging human hippocampus. *Neurobiol. Aging*, 14: 287–293.

Yang, P., Yin, X. and Rutishauser, U. (1992) Intercellular space is affected by the polysialic acid content of NCAM. *J. Cell Biol.*, 116: 1487–1496.

Zoli, M., Jansson, A., Syková, E., Agnati, L.F. and Fuxe, K. (1999) Intercellular communication in the central nervous system. The emergence of the volume transmission concept and its relevance for neuropsychopharmacology. *Trends Pharmacol. Sci*, 20: 142–150.